_____

FINAL REPORT

FIELD TESTING AND CALIBRATION OF THE VERTICAL IN SITU PERMEAMETER (VIP) DEVELOPMENT OF AN IMPROVED VERTICAL AND HORIZONTAL IN SITU PERMEAMETER (VAHIP)

Ana Mohseni
Harald Klammler
Michael Rodgers
Aminta Velasquez
Angelina Liu

January 2020

Department of Civil and Coastal Engineering
Engineering School of Sustainable Infrastructure and Environment
College of Engineering
University of Florida
Gainesville, Florida 32611-6580

DISCLAIMER

The opinions, findings, and conclusions expressed in this publication are those of the author(s) and not necessarily those of the State of Florida Department of Transportation or the U.S. Department of Transportation.

SI (MODERN METRIC) CONVERSION FACTORS (from FHWA)

APPROXIMATE CONVERSIONS TO SI UNITS

SYMBOL	WHEN YOU KNOW	MULTIPLY BY	TO FIND	SYMBOL
LENGTH				
in	inches	25.4	millimeters	mm
ft	feet	0.305	meters	m
yd	yards	0.914	meters	m
mi	miles	1.61	kilometers	km

SYMBOL	WHEN YOU KNOW	MULTIPLY BY	TO FIND	SYMBOL
AREA				
in2	square inches	645.2	square millimeters	mm2
ft2	square feet	0.093	square meters	m2
yd2	square yard	0.836	square meters	m2
ac	acres	0.405	hectares	ha
mi2	square miles	2.59	square kilometers	km2

SYMBOL	WHEN YOU KNOW	MULTIPLY BY	TO FIND	SYMBOL
VOLUME				
fl oz	fluid ounces	29.57	milliliters	mL
gal	gallons	3.785	liters	L
ft3	cubic feet	0.028	cubic meters	m3
yd3	cubic yards	0.765	cubic meters	m3
NOTE: volumes greater than 1000 L shall be shown in m3				

SYMBOL	WHEN YOU KNOW	MULTIPLY BY	TO FIND	SYMBOL
MASS				
oz	ounces	28.35	grams	g
lb	pounds	0.454	kilograms	kg
T	short tons (2000 lb)	0.907	megagrams (or "metric ton")	Mg (or "t")

SYMBOL	WHEN YOU KNOW	MULTIPLY BY	TO FIND	SYMBOL
TEMPERATURE (exact degrees)				
oF	Fahrenheit	5 (F-32)/9 or (F-32)/1.8	Celsius	oC

SYMBOL	WHEN YOU KNOW	MULTIPLY BY	TO FIND	SYMBOL
ILLUMINATION				
fc	foot-candles	10.76	lux	lx
fl	foot-Lamberts	3.426	candela/m2	cd/m2

SYMBOL	WHEN YOU KNOW	MULTIPLY BY	TO FIND	SYMBOL
FORCE and PRESSURE or STRESS				
lbf	poundforce	4.45	newtons	N
kip	kilo poundforce	4.45	kilo newtons	kN
lbf/in2	poundforce per square inch	6.89	kilopascals	kPa

APPROXIMATE CONVERSIONS TO SI UNITS

SYMBOL	WHEN YOU KNOW	MULTIPLY BY	TO FIND	SYMBOL
LENGTH				
mm	millimeters	0.039	inches	in
m	meters	3.28	feet	ft
m	meters	1.09	yards	yd
km	kilometers	0.621	miles	mi

SYMBOL	WHEN YOU KNOW	MULTIPLY BY	TO FIND	SYMBOL
AREA				
mm^2	square millimeters	0.0016	square inches	in^2
m^2	square meters	10.764	square feet	ft^2
m^2	square meters	1.195	square yards	yd^2
ha	hectares	2.47	acres	ac
km^2	square kilometers	0.386	square miles	mi^2

SYMBOL	WHEN YOU KNOW	MULTIPLY BY	TO FIND	SYMBOL
VOLUME				
mL	milliliters	0.034	fluid ounces	fl oz
L	liters	0.264	gallons	gal
m^3	cubic meters	35.314	cubic feet	ft^3
m^3	cubic meters	1.307	cubic yards	yd^3

SYMBOL	WHEN YOU KNOW	MULTIPLY BY	TO FIND	SYMBOL
MASS				
g	grams	0.035	ounces	oz
kg	kilograms	2.202	pounds	lb
Mg (or "t")	megagrams (or "metric ton")	1.103	short tons (2000 lb)	T

SYMBOL	WHEN YOU KNOW	MULTIPLY BY	TO FIND	SYMBOL
TEMPERATURE (exact degrees)				
°C	Celsius	1.8C+32	Fahrenheit	°F

SYMBOL	WHEN YOU KNOW	MULTIPLY BY	TO FIND	SYMBOL
ILLUMINATION				
lx	lux	0.0929	foot-candles	fc
cd/m^2	candela/m^2	0.2919	foot-Lamberts	fl

SYMBOL	WHEN YOU KNOW	MULTIPLY BY	TO FIND	SYMBOL
FORCE and PRESSURE or STRESS				
N	newtons	0.225	poundforce	lbf
kPa	kilopascals	0.145	poundforce per square inch	lbf/in^2

*SI is the symbol for International System of Units. Appropriate rounding should be made to comply with Section 4 of ASTM E380.

TECHNICAL REPORT DOCUMENTATION PAGE

1. Report No.	2. Government Accession No.	3. Recipient's Catalog No.

4. Title and Subtitle	5. Report Date
Field Testing and Calibration of the Vertical In situ Permeameter (VIP) Development of An Improved Vertical and Horizontal In situ Permeameter (VAHIP)	January 2020
	6. Performing Organization Code

7. Author(s)	8. Performing Organization Report No.
Ana Mohseni, Harald Klammler, Michael Rodgers, Aminta Velasquez, Angelina Liu	

9. Performing Organization Name and Address	10. Work Unit No. (TRAIS)
Department of Civil and Coastal Engineering Engineering School of Sustainable Infrastructure & Environment University of Florida 365 Weil Hall – P.O. Box 116580 Gainesville, FL 32611-6580	
	11. Contract or Grant No.
	BDV31-977-23

12. Sponsoring Agency Name and Address	13. Type of Report and Period Covered
Florida Department of Transportation 605 Suwannee Street, MS 30 Tallahassee, FL 32399	Draft Final Report 3/1/16 – 12/30/19
	14. Sponsoring Agency Code

15. Supplementary Notes

Prepared in cooperation with the U.S. Department of Transportation and the Federal Highway Administration

16. Abstract

Hydraulic conductivity (permeability) is a fundamental hydromechanical parameter quantifying the resistance of a permeable medium to water flow. Of interest to FDOT is especially the vertical hydraulic conductivity of the soil underlying stormwater retention ponds, which determines the quickness of stormwater recession (drainage) into the subsurface. In situ measurements of hydraulic conductivity are often considered most accurate and time-effective, because they avoid collection with associated disturbance and subsequent laboratory analysis of soil samples. However, under anisotropic conditions, i.e., when horizontal and vertical conductivities are different, existing field methods are limited to the measurement of an apparent isotropic conductivity, or at best the horizontal conductivity alone. A Vertical and Horizontal In situ Permeameter (VAHIP) was designed and built in the form of a direct-push injection probe with head measurements at the injection screen in addition to two additional head observation points along the probe shaft. Based on existing theory, appropriate pressure transducers were selected with an automated data acquisition system. A PVC probe prototype was designed and fabricated. The prototype was used in laboratory sand barrel tests and FDOT test pit experiments. Based on these results, a steel probe was designed and fabricated, and preliminary field tests were conducted with it. Test pit experiments were complicated by the breaking up of the relatively shallow and loose sand, but successfully demonstrated the functionality of the automated pressure data acquisition. Overall, results from laboratory and field tests confirm the proper working of the probe with sensitivity to separate estimation of horizontal and vertical hydraulic conductivities from injection tests.

17. Key Words	18. Distribution Statement
Vertical In situ Permeameter, Vertical and Horizontal In situ Permeameter, Field Testing, Calibration, Horizontal Conductivity and Vertical Conductivity.	No restrictions.

19. Security Classif. (of this report)	20. Security Classif. (of this page)	21. No. of Pages	22. Price
Unclassified	Unclassified	85	

Form DOT F 1700.7 (8-72)   Reproduction of completed page authorized

ACKNOWLEDGMENTS

EXECUTIVE SUMMARY

Hydraulic conductivity (permeability) is a fundamental hydromechanical parameter quantifying the resistance of a permeable medium to water flow. Of interest to FDOT is especially the vertical hydraulic conductivity of the soil underlying stormwater retention ponds, which determines the quickness of stormwater recession (drainage) into the subsurface. In situ measurements of hydraulic conductivity are often considered most accurate and time-effective, because they avoid collection with associated disturbance and subsequent laboratory analysis of soil samples. However, under anisotropic conditions, i.e., when horizontal and vertical conductivities are different, existing field methods are limited to the measurement of an apparent isotropic conductivity, or at best, the horizontal conductivity alone.

To overcome this limitation, the FDOT has supported a number of research projects in the past to develop a Vertical In situ Permeameter (VIP) and a Vertical and Horizontal In situ Permeameter (VAHIP). Typical problems encountered in those studies included the clogging of injection screen slots, mechanically complicated probe designs, difficulty in driving the probe to larger depths, and establishing a physically sound method for interpreting test results in terms of horizontal and vertical conductivities. Several of these problems could be overcome with the latest design of the VIP using a retractable probe tip for injection. It was extensively validated during a FDOT project at different field sites, where independent conductivity estimates from common borehole tests were available for comparison. However, the VIP only provides an apparent mean value of permeability under anisotropic conditions instead of values for vertical and horizontal permeability individually. Moreover, the VIP probe is difficult to drive into the ground to depths exceeding approximately 3 m, requiring temporary removal of the probe for time-consuming pre-drilling.

For this reason, the present project focuses on the construction and testing of a new probe configuration which may be constructed at smaller diameter and without lateral wings, thus reducing resistance to pushing down to larger depths. This new design allows for measurement of horizontal and vertical conductivities from a single injection, based on potential flow theory. It reduces or eliminates effects of screen smearing and / or partial clogging by using two head observations along the probe casing, and not possessing any complicated moving parts inside the probe as currently required for the VIP's tip opening and closure. Hence, the Vertical and Horizontal In situ Permeameter (VAHIP) is a direct-push injection probe with head measurements at the injection screen in addition to two additional head observation points along the probe shaft. Based on existing flow theory and expected pressures, appropriate pressure transducers were selected with an automated data acquisition system. A PVC probe prototype was designed and fabricated. The prototype was used in laboratory sand barrel tests and FDOT test pit experiments. Based on these results, a steel probe was designed and fabricated, and preliminary field tests were conducted with it.

A search was conducted among several manufacturers offering pressure transducers for groundwater applications with maximum ranges of approximately 30 psi or 20 m of water column. Other important selection criteria included accuracy, submergibility, and small size for minimizing overall probe diameter. This resulted in the choice of the model MTM3000, which is a stainless-steel by PMC Engineering, fully submersible pressure transducer with an accuracy of 2 cm (0.1 % full scale), diameter of 1 cm, and length of 9 cm. In addition, a commercial mobile power supply

unit was selected to supply the three transducers during laboratory, test pit, and field experiments by providing the required excitation voltage of 15-30 VDC.

A hollow steel rod with an external diameter of 4.45 cm was chosen to form the body of the probe. This is exactly equal to the outer diameter of AWJ rods used to connect the probe to an SPT (Standard Penetration Test) rig, while still accommodating the chosen transducers inside. The VAHIP has a conical tip of 60° to facilitate driving the probe into the subsurface and was designed to have a single lateral injection screen of 4 cm in length with two head observation locations along the casing at 4 and 20 cm from the lower end of the screen. For each observation head, four observation holes (every 90°) with a diameter of 0.64 cm around the circumference were drilled. Porous stones surrounding the ports allow pressure communication between soil and observation chambers, while preventing the intrusion of soil particles. Three pressure transducers were deployed (behind injection screen plus two observation chambers) using impermeable rubber packers to hold them in place and simultaneously hydraulically isolating them mutually (i.e., avoid water flow inside the probe between chambers).

For the laboratory and test pit experiments, a simplified PVC prototype was constructed with internal and external diameters of 3.5 cm and 4.2 cm, respectively. Laboratory testing was performed using three custom-packed sand barrels to emulate different degrees of anisotropy in hydraulic conductivity. This was achieved by packing one barrel uniformly with sand, while the other barrels were packed using different degrees of layering between sand and a thin, but less permeable, geotextile. Thus, the presence of the geotextile significantly reduced the vertical conductivity, while barely affecting the horizontal conductivity. The laboratory testing served to successfully verify the proper performance of the chosen VAHIP design by comparing VAHIP estimates of horizontal and vertical conductivities for all three anisotropy scenarios with independent conductivity measurements using separate horizontal and vertical flow experiments (i.e., direct measurements).

Subsequently, several injection tests were performed in the test pit facility at the Florida Department of Transportation (FDOT) using the VAHIP PVC prototype. The test pit experiments served to successfully validate the compatibility of the probe with FDOT field gear, such as injection vessel, hose and data acquisition, including laptop connection and real-time monitoring. The interpretation of test results was complicated by frequent breaking-up of the soil near the probe and resulting distortions of the flow field and pressure measurements. This may be attributed to the installation procedure for the PVC prototype requiring pre-augering and then back-filling soil around the probe, as well as the very shallow installation depths. However, both issues are pure artifacts of the experimental configuration (i.e., PVC probe and test pit) and can be ruled out for actual field applications using the driven steel probe.

Finally, the steel version of the VAHIP was manufactured, and a number of field injection tests were performed in the backyard of the FDOT State Materials Office. The field test location was chosen for proximity and its known shallow groundwater table next to a stormwater retention pond containing surface water. The probe was successfully installed multiple times to variable depths by continuous driving using the FDOT drill rig. Preliminary test results at the last location yielded a horizontal conductivity of 6.7×10^{-07} m/s and a vertical conductivity of 9.6×10^{-07} m/s. Due to these relatively low conductivities, the soil was classified as silty or clayey, which is reasonable for the

test site. The values of horizontal and vertical conductivities are very close, indicating that the test soil may be relatively isotropic.

Overall, results from laboratory and field tests confirm the proper working condition of the probe with sensitivity to separately estimate horizontal and vertical hydraulic conductivities from injection tests. Possible limitations that may require further attention include effects of soil clogging, which could not be completely removed with the new VAHIP, and the loosening of the rubber stoppers holding the pressure transducers, which could create small but undesirable flow connections between pressure observation chambers.

Table of Contents

LIST OF TABLES

LIST OF FIGURES

CHAPTER 1

1. IDENTIFICATION OF AN APPROPRIATE PRESSURE MEASUREMENT SYSTEM

A small and accurate pressure transducer was needed for developing a probe to measure in situ permeability. Also, a data-acquisition and transmission system to take real-time readings of the transducers in the field was selected.

1.1 PRESSURE TRANSDUCER SELECTION

A pressure transducer is a device that detects pressure from gases or liquids and converts it into an analog electrical signal (voltage, current, or frequency). Most instruments consist of a sensitive diaphragm which is subjected to deformation due to the fluid pressure. This again results in strain in the gages that are bonded to it, which causes a change in electrical resistance proportional to the applied pressure.

1.1.1 Selection Criteria

A search was conducted including several manufacturers offering pressure transducers for groundwater applications for measurement ranges of approximately 30 psi or 20 m of water column. An initial tentative probe design had an external diameter of 5 cm (similar to older VIP/VAHIP probes), therefore limiting the transducer diameter to 4.5 cm. The comparison of pressure transducers for this design criterion can be found in Table 1-1. The second and current probe design has a smaller external diameter of 3.73 cm, with an internal diameter of 1.6 cm. Table 2 shows the transducer options that would fit this design. The reduced probe diameter corresponds to that of CPT-u (Cone Penetration Test) probes currently used by DOT (Department of Transportation) and is expected to allow for easier driving (and possibly hammering) to greater depths without pre-drilling. Besides size limitations, the selection process was based on additional aspects like water resistance, measurement range, accuracy and reliability.

From Table 1-2, it can be seen that some of the pressure transducers are submersible, and the rest have an IP66, IP67, and IP68 ingress protection classification (IP66 corresponding to a lower protection against intrusion of liquids, compared to IP67, and IP68). For example, the EPB-PW pressure transducer is rated as an IP68. According to the manufacturer, this means that it would resist up to 10 meters of immersion during a limited period of time. For the purpose of this project, however, this would result in a constraint for the probe by limiting the maximum depth and injection pressures. Consequently, pressure transducers rated IP66, IP67, and IP68 were not considered further. This reduces the options to two fully submersible pressure transducers: the FOP MicroPZ with ±1.0% FS (full span or measuring range) accuracy and the MTM3000 with ±0.1% FS accuracy. Based on better accuracy, the MTM3000 was chosen.

The manufacturer PMC Engineering offers the selected Miniature MTM3000 Series of submersible transmitters. The transducer possesses a high stability piezoresistive silicon chip as the sensor element that is isolated from the process media with an isolation diaphragm. Its body consists of a cylindrical titanium case with a diameter of 0.99 cm and a length of 8.64 cm (Figure

1), which is suitable for the conditions in which the new VAHIP is planned to be used. The specifications of the MTM3000 can be seen in Table 3.
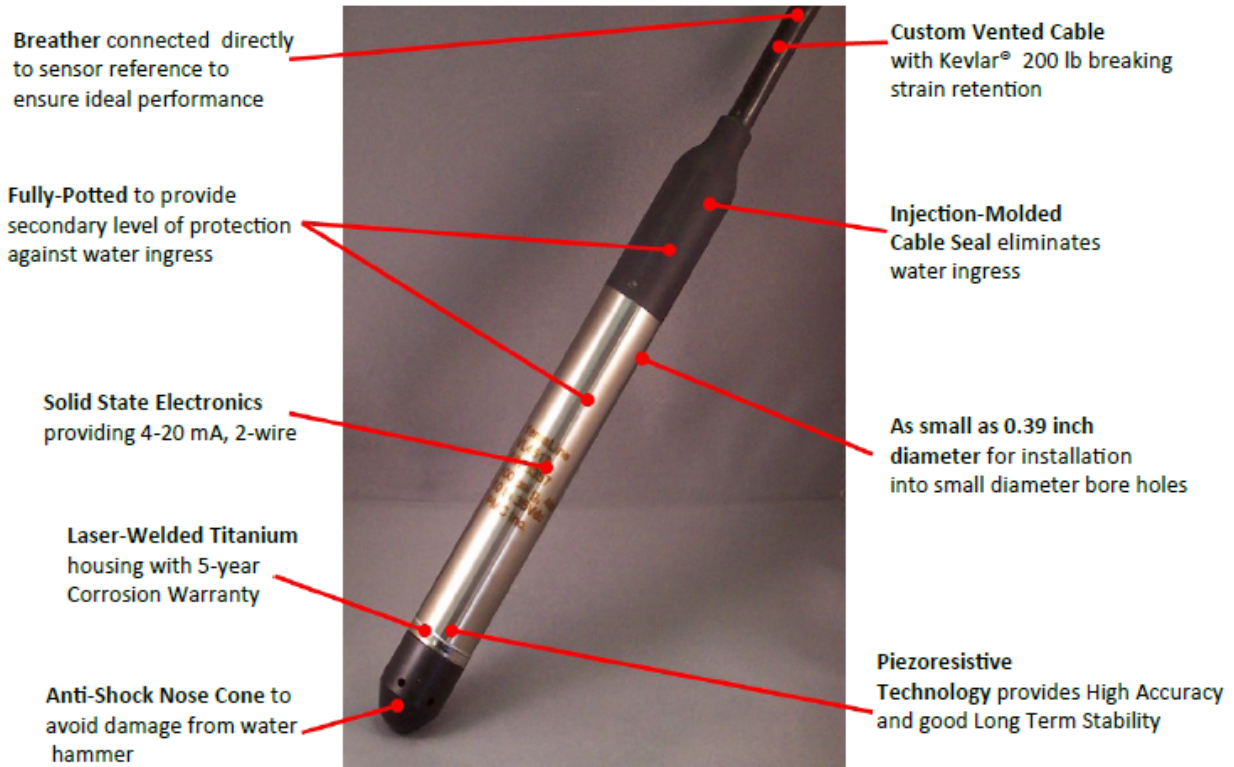
Figure 1.1. Miniature MTM3000 Series submersible transmitter

The specifications revised for the options were:

1.1.1.1 Accuracy

Accuracy is defined as the closeness between the pressure transducer's reading and the actual value, sometimes this value is expressed as a percentage of the reading, as an absolute value or as a percentage of span. For the MTM3000, the accuracy stated by the manufacturer is ±0.1% FS, in this case the full span is 30 psia, which means that the measured value of pressure would be accurate to ±0.03 psia. Some manufacturers include the effects of non-linearity, hysteresis, and repeatability in the accuracy.

Table 1.1 Comparison of pressure transducers with larger diameters

Specifications	Models							
	PK20S	HD-PK45S	PWS	PWF	VW2100	VW2100-HD	VW2100-L	VW2100-LV
Measuring range	24.66 psi	24.66 psi	29.01 psi	29.01 psi	50.76 psi	50.76 psi	25.38 psi	25.38 psi
Accuracy	<0.25% FS	<0.25% FS	±0.1%	±0.1%	±0.1%	±0.1%	±0.1%	±0.1%
Ingress Protection	Submersible	Submersible	Submersible	Submersible	Submersible	Submersible	Submersible	Submersible
Material	Stainless steel	Stainless steel	Stainless steel	Stainless steel	Stainless steel	Stainless steel	Stainless steel	Stainless steel
Diameter	20 mm	28 mm	19 mm	28.6 mm	19 mm	25.4 mm	25 mm	25 mm
Length	180 mm	200 mm	200 mm	200 mm	130 mm	146 mm	133 mm	133 mm
Price	$ 268.00	$ 398.00	$ 306.00	$ 306.00	$ 440.00	$ 612.00	$ 714.00	$ 1,020.00

Table 1.1 (continued). Comparison of pressure transducers of larger diameters

Specifications	Models							
	Standard	Heavy duty	Low pressure	KPA	KPB	KPC	KPD	M5600
Measuring range	50 psi	50 psi	25 psi	29.01 psi	29.01 psi	29.01 psi	29.01 psi	50 psi
Accuracy	±0.1% FS	±0.1% FS	±0.1% FS	±0.1%	±0.1%	±0.1%	±0.1%	±0.25% FS
Ingress Protection	Submersible	Submersible	Submersible	IP68	IP68	IP68	IP68	IP66-IP67
Material	Stainless steel	Stainless steel	Stainless steel	Stainless steel	Stainless steel	Stainless steel	Stainless steel	Stainless steel and polycarbonate
Diameter	19 mm	29 mm	29 mm	40 mm	40 mm	30 mm	30 mm	27.69 mm
Length	155 mm	191 mm	191 mm	84 mm	142 mm	77 mm	120 mm	
Price	$ 409.00	$ 582.00	$ 468.00	$ 710.00	$ 766.00	$ 694.00	$ 750.00	$ 190.40

Table 1.2 Comparison of pressure transducers with smaller diameters

Specifications	Models							
	EPB-PW	EPRB-1	EPRB-3	XP5	XPM4	XPR46	FOP MicroPZ	MTM3000
Measuring range	25 psi	50 psi	50 psi	30 psi	75 psi	30 psi	30 psi	30 psi
Accuracy	±1.0% FS	±0.25% FS	±0.25% FS	±0.5%-1% FS	±0.35%-0.95% FS	±1% FS	±1.0% FS	±0.1% FS
Ingress Protection	IP68	IP66	IP66	IP67	IP67	IP66	Submersible	Submersible
Material	Titanium	Stainless steel	Stainless steel	Titanium	Titanium	Titanium	Stainless steel	Stainless steel
Diameter	6.4 mm	12.7 mm	13.86 mm	11.55 mm	9.24 mm	4.6 mm	4.8 mm	9.91 mm
Length	11.4mm						54 mm	86.36 mm
Price				$ 1,051.20			$ 590.00	$ 898.88

1.1.1.2 Linearity

Linearity is the degree of proportionality between the actual measured curve of a sensor and the ideal curve over the full scale of the sensor.

1.1.1.3 Hysteresis

It can be defined as the maximum difference in sensor output at a pressure when that pressure is approached first with an increasing followed with a decreasing measurand during a full span pressure cycle.

1.1.1.4 Repeatability

Is defined as the sensor's ability to provide the same results for a certain number of readings when the same pressure is applied under identical conditions.

1.1.1.5 Type of Pressure Measurements

For the selected model of pressure transducer, the options were gage and absolute pressure. Gage pressure measurements are with respect to the atmospheric pressure at the vent tube of the instrument, therefore the readings shown will be 1 atm less than the absolute pressure. Absolute pressure is zero-referenced against a perfect vacuum, so the readings from the transducer are always positive. The absolute pressure type was selected because the goal is to measure pressure changes due to injection, which are independent of atmospheric pressure, and because this type does not require vent tubes connected to the atmosphere, which would complicate design.
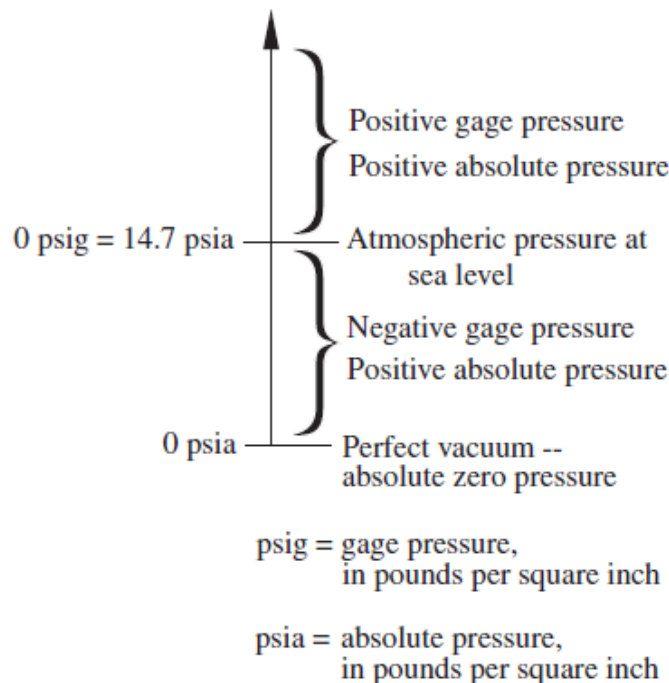
Figure 1.2 Difference between absolute pressure and gauge pressure for a location at sea level

5

Table 1.3 MTM 3212 pressure transducer specifications

DESCRIPTION	SPECIFICATION
Range	0-30 psia
Diameter	0.39 in
Accuracy	±0.1% F.S. Includes non-linearity, hysteresis, repeatability
Overpressure	3 x full scale range
Operating temperature	-4°C to 50°C (25°F to 125°F)
Compensated Temperature	-2°C to 30°C (30°F to 85°F)
Temperature Effects (Compensated)	±2% total for 25°F to 125°F
Long term stability	0.1% FS per year
Electrical VDC	(3 wire) from 15-30 VDC supply
Electrical configuration	0-10 Volts
Cable	Polyurethane molded, vented with Kevlar, 6 conductors
Housing	Titanium standard with 5-year corrosion warranty
Weight	1 oz. (excluding cable)

1.2   DATA-ACQUISITION TRANSMISSION SYSTEM SELECTION

A commercial mobile power supply unit was selected to power the three transducers in the field, and the required excitation voltage for the transducer is 15-30 VDC.

Commercial voltmeters will be used for reading transducer signals in real-time above ground with an accuracy equal or smaller than the ±0.1% accuracy of the transducers.

CHAPTER 2

2. DEVELOPMENT OF COMPUTER-AIDED DRAWINGS (CAD)

This chapter will provide details about the Vertical and Horizontal In situ Permeameter such as design, drawings detailing dimensions and corresponding connections to ensure the correct performance and configuration of the probe in the field.

2.1   VAHIP DESIGN

The probe consists of a hollow steel rod with an external diameter of 4.45 cm (Figure 1) which is the outer diameter of AWJ rods used to connect the probe to a SPT rig. The VAHIP has a conical tip of 60° to facilitate driving the probe into the subsurface and was designed to have a single injection screen (records injection head) with two head observations along the casing. For each observation head, four observations ports (every 90°) with a diameter of 0.64 cm around the circumference were used. Porous stones surround the ports to allow water entering into the observation chambers when the probe is pushed below the ground water table, and also to prevent soil particles intrusion. In order to measure hydraulic heads due to injection, three pressure transducers were used in the design (Figure 2).

The probe is formed by five threaded sections to facilitate the transducers placement:

1. The bottom section consists of the conical tip and the bottom observation chamber. The bottom observation ports are located at $t_2 = 22.23$ cm from the screen end, as depicted in Figure 3. Above the ports, a rubber stopper is placed to hydraulically isolate the bottom and middle chambers while keeping the transducers in place.
2. The next section (Figure 4) was added to decreased the volume of the middle observation chamber and allow for a faster filling process once the probe has reached the water table.
3. The middle section records another observation head with ports located at $t_1 = 4.45$ cm from the edge of the screen as shown in Figure 5.
4. The injection chamber has a 4.45 cm long injection screen that possesses three sections around the circumference, with nine horizontal slots each (Figure 6). The vertical distance between slots is 0.46 cm and the slot thickness is 0.81 mm. A rubber stopper is needed at the top to hold the top pressure transducer. Additionally, the stopper has a hole to allow the injected water to flow down and exit through the screen
5. The upper section was designed to attach an AWJ adaptor to the top of the probe (Figure 7), allowing it to be pushed into the ground using an SPT rig.

To maximize the sensitivity to anisotropy based on Klammler et al. (2017), values of $t_1/s \leq 1$ and $t_2/s \geq 5$ were selected, where s is the screen length. According to the VAHIP geometry $t_1/s = 4.45/4.45 = 1 \leq 1$ and $t_2/s = 22.23/4.45 = 5 \geq 5$.

The original CAD drawings shown in Figure 2.1 through Figure 2.7.
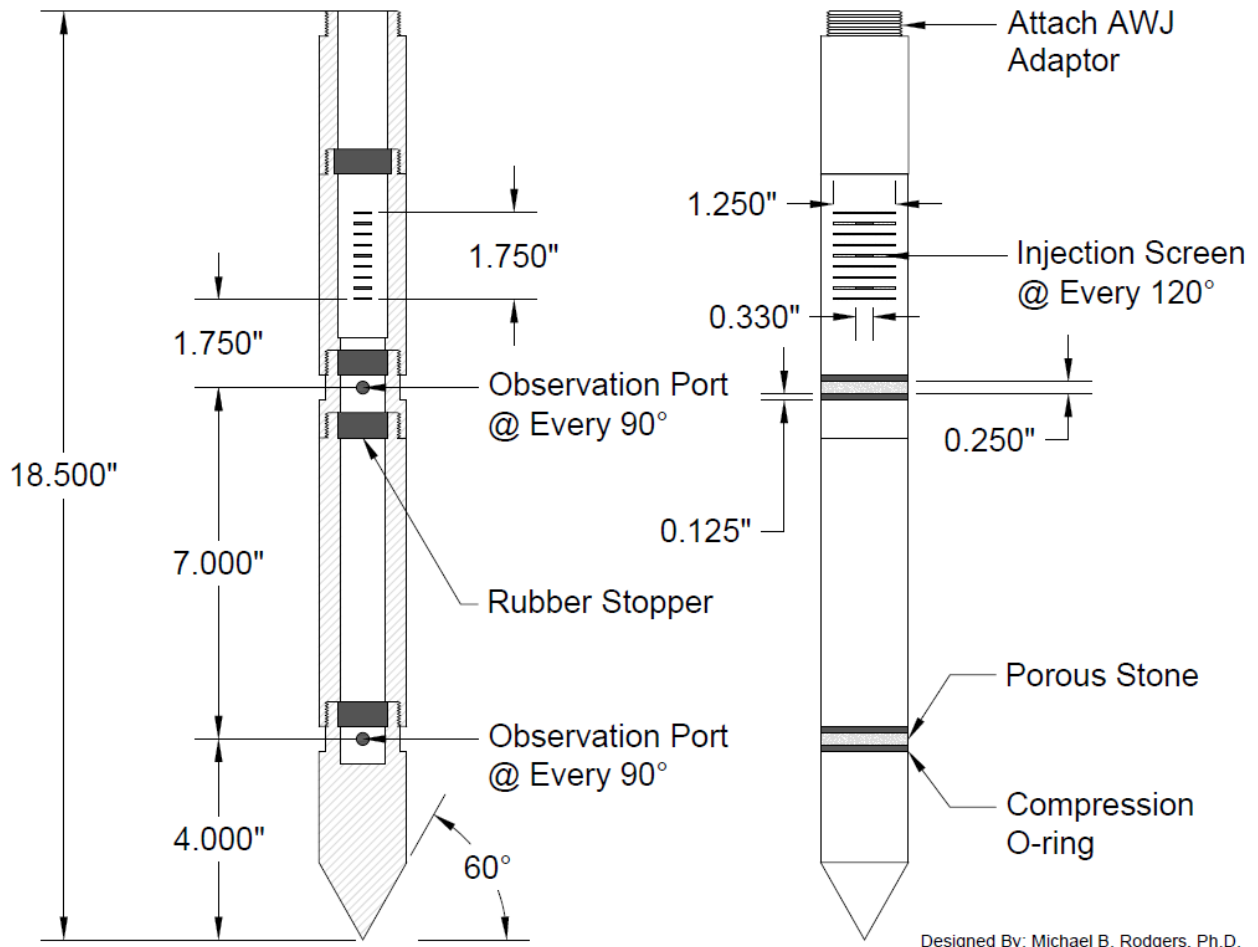
Figure 2.3 VAHIP design and dimensions.
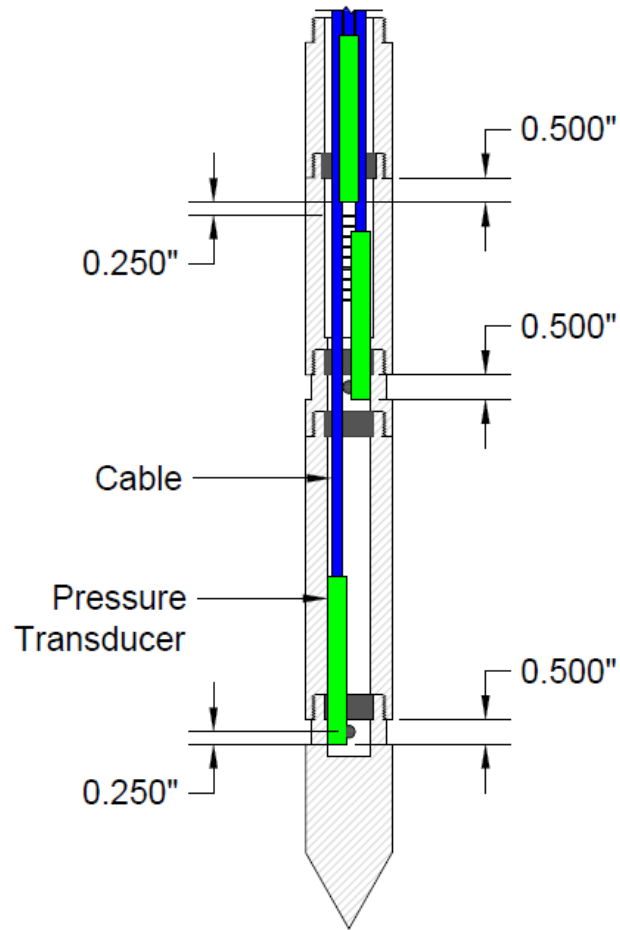
Figure 2.4 Transducers location inside of the VAHIP
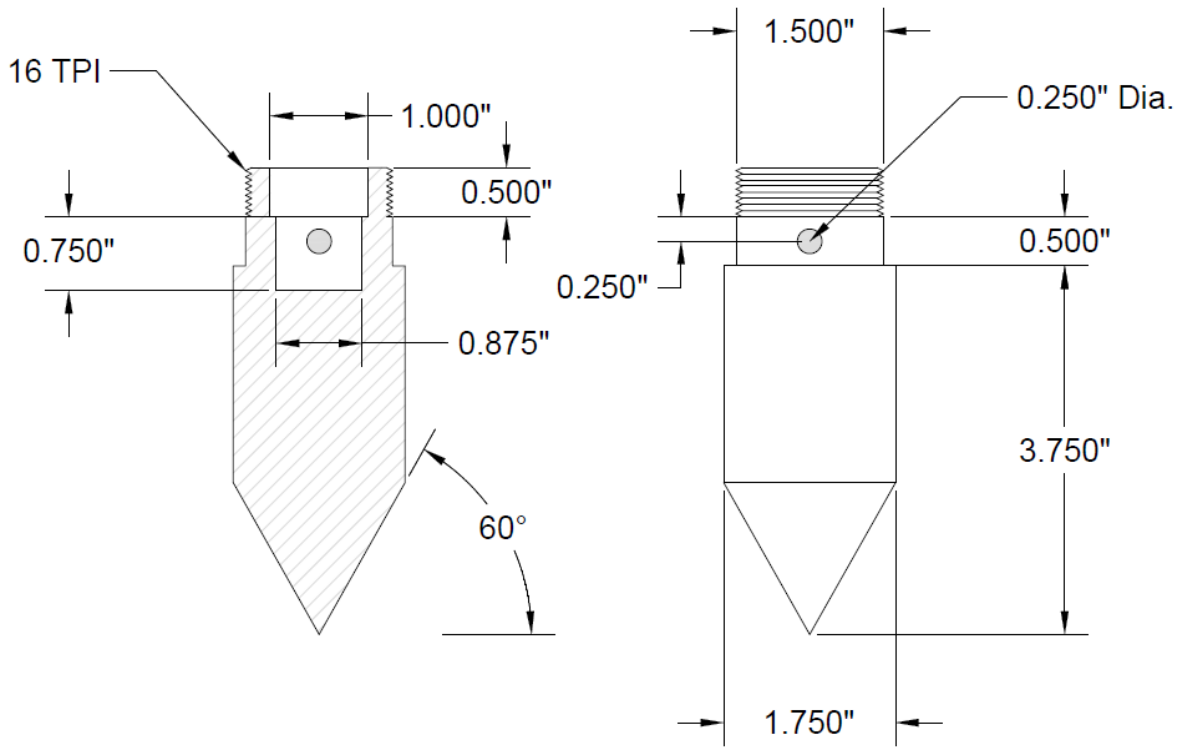
Figure 2.5 VAHIP bottom observation chamber
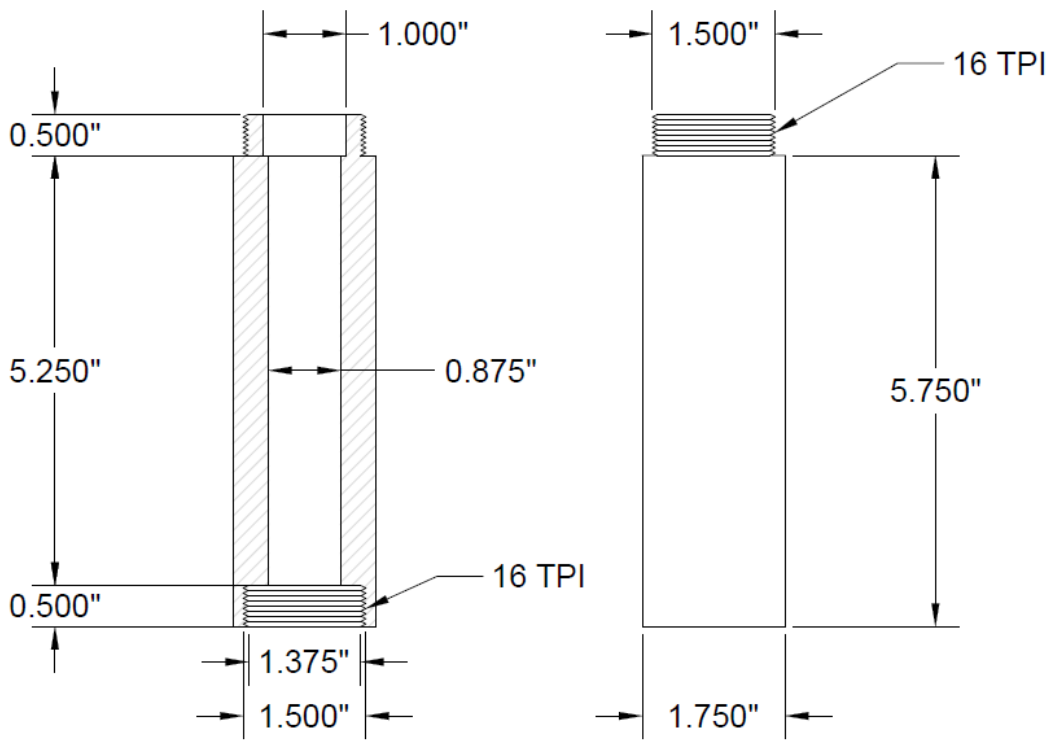
Figure 2.6 VAHIP section to reduce volume of middle chamber
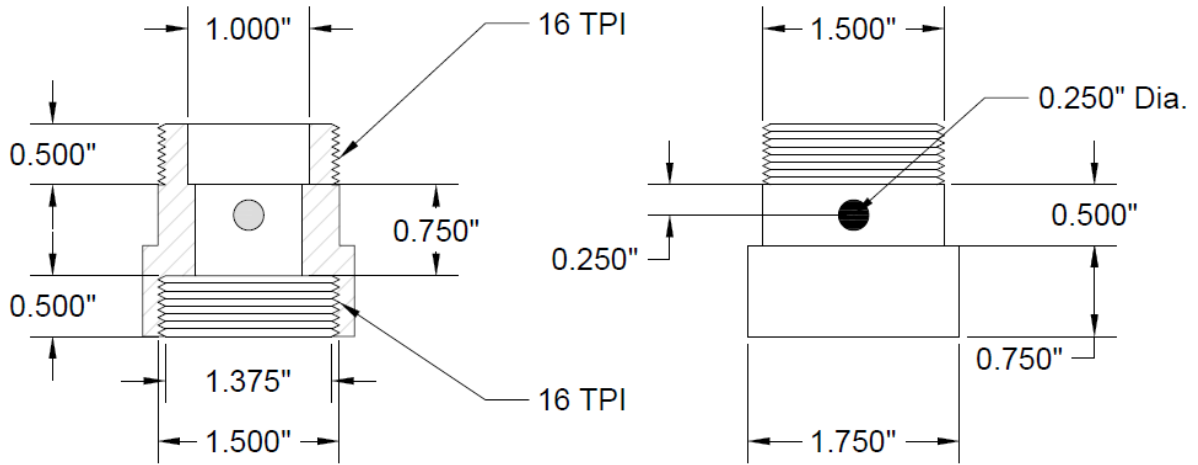
Figure 2.7 VAHIP middle observation chamber
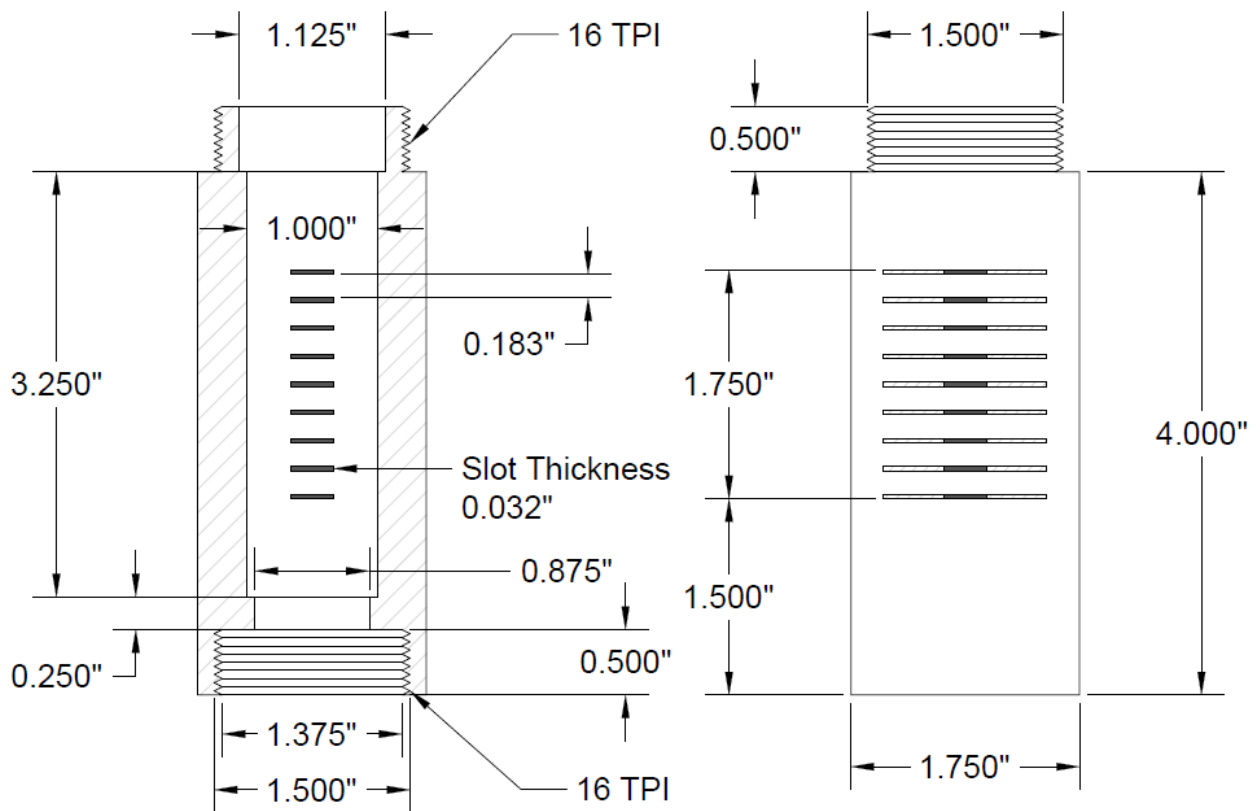
Figure 2.8 VAHIP injection chamber

11
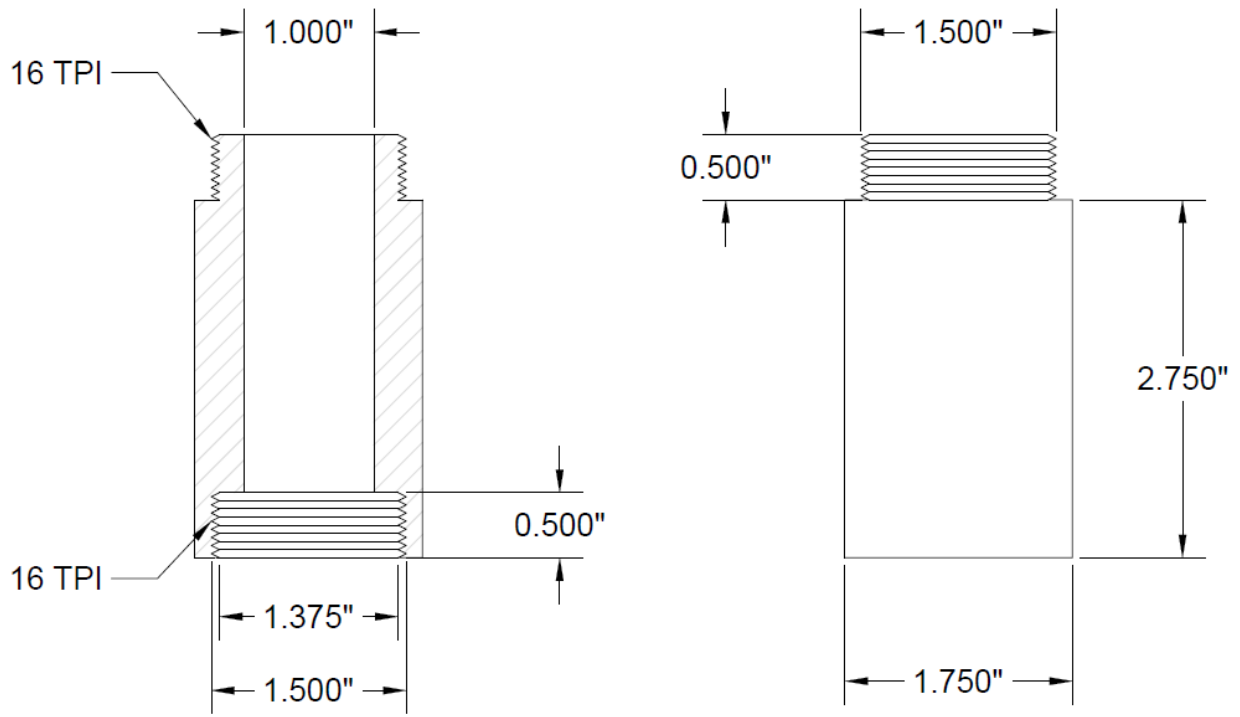
Figure 2.9 VAHIP top section

CHAPTER 3

3. FABRICATION OF A PVC-PROTOTYPE

3.1 OBJECTIVES

Based on the VAHIP design, consisting of a single injection port with two head observations along the probe, a prototype was developed in order to achieve the following objectives.

- Test and calibrate the pressure transducers used in the design.

- Validate the Klammler et al. (2011) semi-analytical method to estimate horizontal and vertical components of hydraulic conductivity.

- Adjust the probe design or injection mechanism according to conclusions from laboratory testing.

- Ensure the correct performance and configuration of the probe in the field.

3.2 VAHIP PVC-PROTOTYPE

A PVC prototype was developed with an internal and external diameter of 3.5 cm and 4.20 cm, respectively. The design and dimensions were depicted in Figure 3.1. Inside of the PVC pipe are three rubber stoppers that were drilled to allow the transducer's cables to pass upward. The assembled and disassembled prototype can be seen in Figure 3.2. Additionally, each of the three pressure transducers is held in place by a stopper while creating three separate chambers hydraulically isolated from each other.

The upper chamber was designed to inject water into the surrounding soil and possesses a 4-cm-long screen. The screen consists of three sections around the circumference where each section possesses nine horizontal slots with 0.5-mm to 1-mm thickness, with the vertical distance between slots being 0.5 cm. The stopper on the top has a 1.26-cm² hole to allow the injected water to flow downward and exit through the injection zone. The upper transducer measures the injection head φ_0.

The middle and bottom chamber are for head observations. Below each rubber stopper, four holes of 0.56 cm in diameter were drilled around the circumference to allow water to enter the observation chambers. A permeable fabric covers each hole to prevent soil particles entering the chambers. Each pressure transducer measures the observation head in its corresponding compartment. The middle transducer records the observation head φ_{t1} located at $t_1 = 4$ cm from the screen bottom to the observation ports in the middle chamber. The bottom transducer records φ_{t2} located at $t_2 = 20$ cm from the screen end to the observation ports in the bottom chamber.

Each section of the probe (Figure 3.3) is connected through PVC couplings to facilitate the rubber stoppers and transducers placement inside the PVC pipe. On top of the probe, a quick connect was used to inject water while having a sealed connection to avoid air from entering the system (Figure

3.4). Therefore, the transducers cables were passed through a rubber stopper located at the side of the probe.
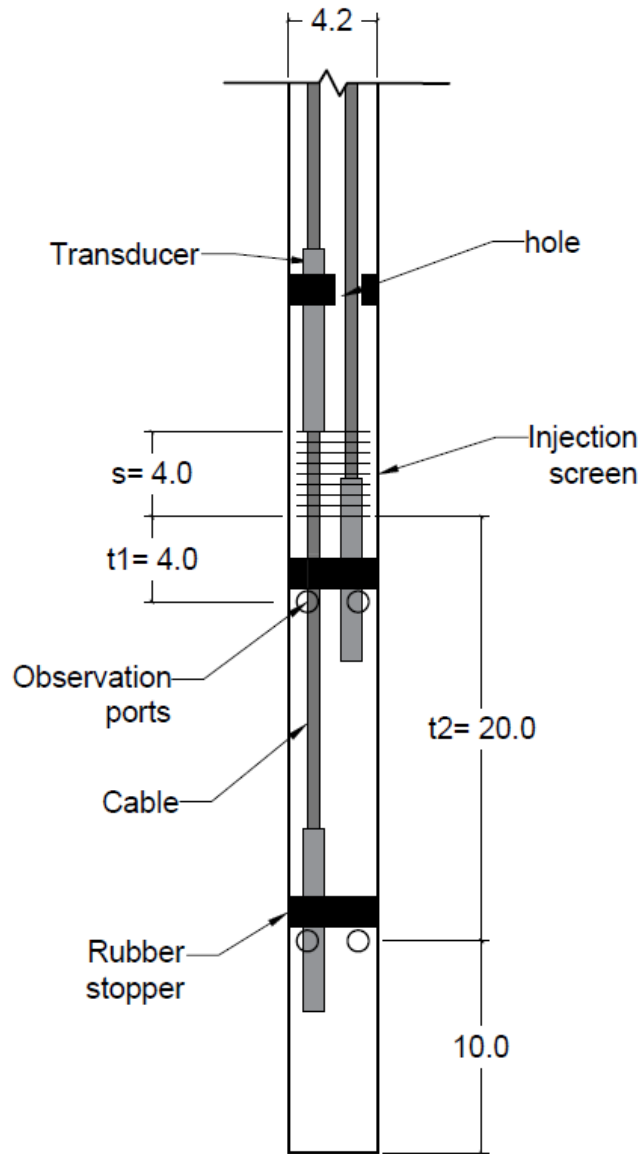
Figure 3.10 PVC-prototype design in cm (not to scale)

The probe geometry was selected to maximize the sensitivity to anisotropy based on Klammler et al. (2017), where the paper suggests values for $t_1/s \leq 1$ and $t_2/s \geq 5$. Following these recommendations, the PVC prototype was designed with values of $t_1/s = 4/4 = 1 \leq 1$ and $t_2/s = 20/4 = 5 \geq 5$. The tip length from the bottom observation port is a few times longer than the probe diameter. Moreover, the radius of the PVC prototype (a= 2.1 cm) is similar to that of CPT-u probes and is expected to provide less resistance when driving the probe into the ground.

Figure 3.11 Assembled prototype on the left and disassembled on the right

Figure 3.12 Upper, middle, and bottom chamber (from left to right)

Figure 3.13 Quick connection at the top of the probe

CHAPTER 4

4. LABORATORY TESTING AND RESULTS

Several injection tests in sand-packed barrels using the VAHIP PVC prototype under saturated conditions were performed to compare both horizontal and vertical permeability estimates to a widely used constant head tests for perfectly horizontal and vertical flow. Moreover, preliminary and laboratory tests were essential in order to accomplish the following objectives:

- Calibrate the three pressure transducers and verify the readings were within the error range specified by the manufacturer;
- Verify the proper performance of the PVC prototype;
- Modify the testing procedures based on issues encountered in laboratory tests;
- Test the PVC prototype in different scenarios with varying anisotropy created by layering of the sand-packing in the barrel;
- Compare test results.

4.1   CALIBRATION OF PRESSURE TRANSDUCERS

The three pressure transducers described previously were calibrated by submerging them inside of a water-filled PVC pipe and recording the readings provided by the voltmeters every 1 cm and then every 5 cm, with the maximum depth tested being 1 m. When converting the output signal into height of water and comparing to submerged depths, it was observed that the error in the readings was within the error specified by the manufacturer (i.e., ±2.1 cm). Additionally, the transducers were calibrated inside the PVC prototype, where pressures were recorded while the probe was being submerged every 5 cm until a depth of 1.35 m was reached. However, larger errors than the stated by the manufacturer were observed for the top transducer based on the change in voltage with respect to the transducer voltage out of water. This issue is neglected if the change in pressure between consecutive readings is taken.

4.2   ANISOTROPY SCENARIOS

The permeability tests were performed in three different anisotropy scenarios.
1. Scenario 1: coarse sand only.
2. Scenario 2: 1 cm of coarse sand intercalated between one layer of fabric (thickness around 0.055 cm), which was less permeable than the sand.
3. Scenario 3: 1 cm of coarse sand intercalated between two layers of fabric (same fabric used for the scenario 2).

Anisotropy was simulated for the layered scenarios, where horizontal layers of sand and fabric were used. The relatively low conductivity of the fabric diminished the vertical flow, while the horizontal flow increased through the sand layers due to its higher conductivity. Due to the fact that for scenario 3 two layers of fabric were placed between sand, this was the scenario with the highest difference between horizontal and vertical conductivities.

An equivalent conductivity can be computed with Equation 4-1 for layered scenarios where flow is applied parallel to the layers. And Equation 4-2 can be used for flow perpendicular to the layers.

$$k_{h(eq)} = \frac{n_{sand}d_{sand}k_{sand} + n_{fabric}d_{fabric}k_{fabric}}{n_{sand}d_{sand} + n_{fabric}d_{fabric}} \qquad (4\text{-}1)$$

$$k_{v(eq)} = \frac{n_{sand}d_{sand} + n_{fabric}d_{fabric}}{\dfrac{n_{sand}d_{sand}}{k_{sand}} + \dfrac{n_{fabric}d_{fabric}}{k_{fabric}}} \qquad (4\text{-}2)$$

where, n_{sand} and n_{fabric} are the number of layers, d_{sand} and d_{fabric} are the thickness of each layer (L), and k_{sand} and k_{fabric} are the hydraulic conductivity of sand and fabric respectively (L/T).

4.3   INDEPENDENT HORIZONTAL FLOW TEST (CONSTANT HEAD TEST)

Preliminary small-scale tests in rectangular boxes were performed to obtain independent measurements of horizontal conductivity for comparison to injection tests. Constant head tests were performed for the three scenarios previously mentioned. Additionally, gravel was placed at both sides of the material being tested (Figure 4.1 and Figure 4.2), for which a metallic mesh was needed along with a permeable fabric in order to keep the sand out of the gravel sections. The sand was wet-packed into the box to avoid trapped air in the sample. The same packing process for each scenario was used for the barrel tests (in which injection tests were performed using the VAHIP prototype) to replicate the same conductivities. Furthermore, horizontal flow was imposed (parallel to the layers) to compute horizontal conductivity using Equation 4-3.

$$k_h = \frac{2QL}{w\,(h_u^2 - h_d^2)} \qquad (4\text{-}3)$$

where, L = length of sample (L), w = width of sample in the direction perpendicular to flow (L), h_u = up-gradient water level (L), and h_d = down-gradient water level (L).
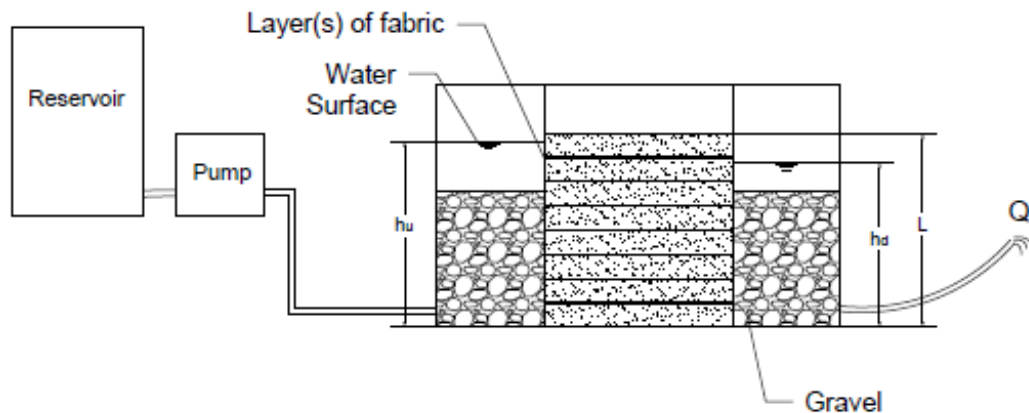
Figure 4.1 Horizontal flow permeability test for layered scenarios

18

Figure 4.2 Horizontal flow permeability test

The results of the horizontal conductivity tests can be seen in Table 4.1 through Table 4.3, where the estimates of k_h increase with the number of layers of fabric. Moreover, Q was plotted against $w(h_u^2-h_d^2)/2L$ (Figure 4.3) for the three scenarios, where the slope of each trendline corresponds to the horizontal conductivity obtained using a linear regression. The coefficient of determination for each trendline was high.

Table 4.1 Horizontal conductivity results for scenario 1, w = 20 cm

h_u (cm)	h_d (cm)	Q (cm³/s)	k_h (cm/s)	$k_{h, average}$ (cm/s)
13.05	11.95	0.88	0.052	
13.00	12.00	0.75	0.049	
12.80	11.60	1.02	0.057	
13.25	11.00	3.11	0.070	
13.25	11.00	3.05	0.068	0.069
15.10	14.35	1.44	0.071	
13.95	12.60	2.04	0.062	
13.35	11.65	2.24	0.058	

Table 4.2 Horizontal conductivity results for scenario 2. In total, 13 layers of fabric and 14 layers of sand were used. L = 14.72 cm and w = 20 cm

h_u (cm)	h_d (cm)	Q (cm³/s)	k_h (cm/s)	$k_{h, average}$ (cm/s)
15.45	13.05	8.44	0.18	
15.45	12.35	7.45	0.13	
15.25	11.85	7.07	0.11	
14.05	10.30	7.16	0.12	
13.95	13.05	2.47	0.15	0.14
13.75	12.75	2.68	0.15	
13.45	12.40	2.58	0.14	
12.25	10.90	2.83	0.13	

Table 4.3 Horizontal conductivity results for scenario 3. In total, 26 layers of fabric and 14 layers of sand were used. L = 15.43 cm and w = 20 cm

h_u (cm)	h_d (cm)	Q (cm³/s)	k_h (cm/s)	$k_{h, average}$ (cm/s)
11.90	11.45	1.10	0.16	
12.85	11.70	3.21	0.18	
11.45	10.35	3.42	0.22	
15.40	12.70	7.82	0.16	
13.30	11.05	5.80	0.16	0.17
14.05	12.15	5.42	0.17	
14.55	13.30	3.98	0.18	
14.10	13.15	2.82	0.17	
13.20	12.85	0.99	0.17	
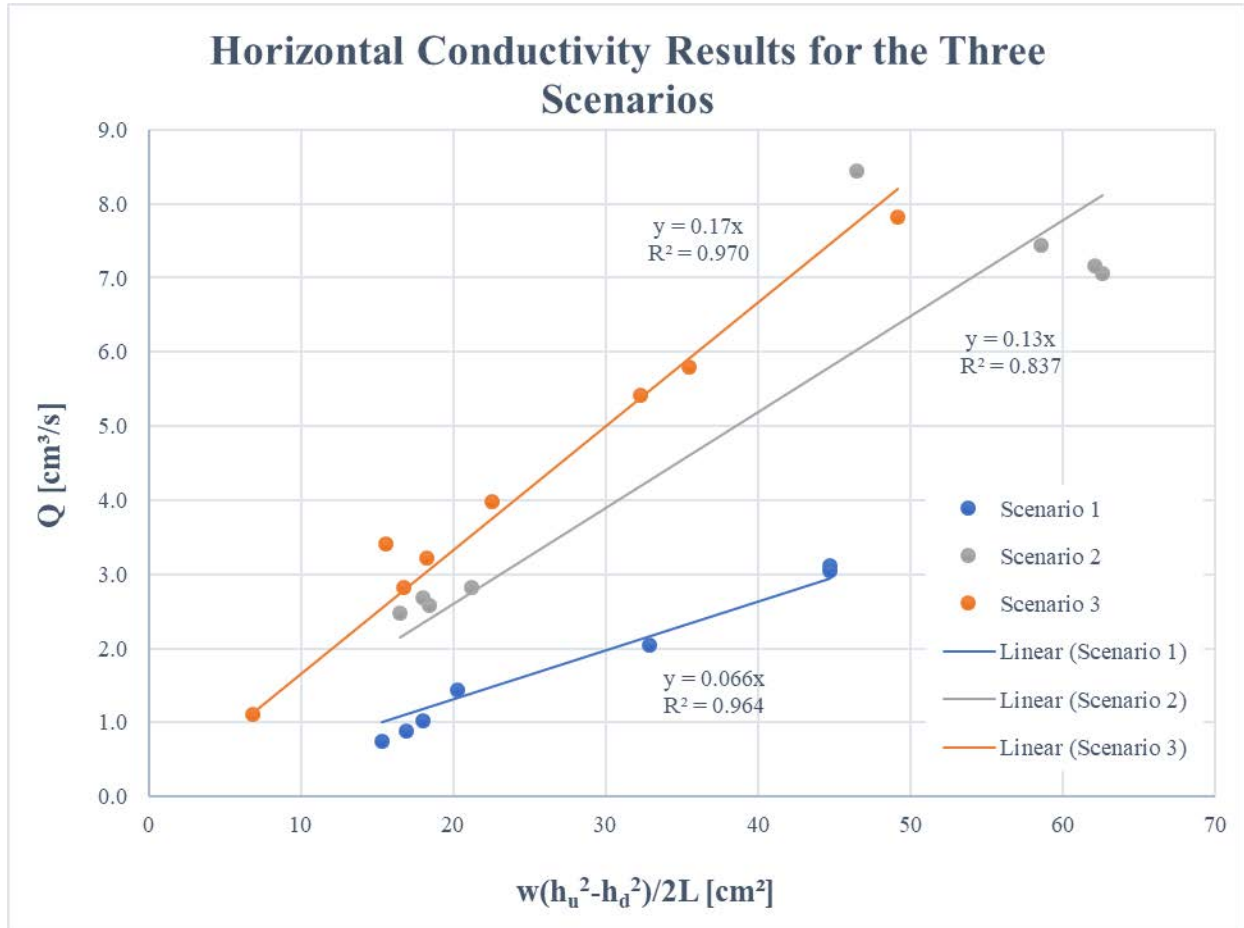
Figure 4.3 Flow rate Q as a function of w(hu2-hd2)/2L for the three anisotropy scenarios.

4.4   INDEPENDENT VERTICAL FLOW TEST (CONSTANT HEAT TEST)

To estimate the vertical permeability a 55-gallon barrel was used, and the diameter of the barrel was 55.4 cm. The sand was wet-packed on top of 12.4 cm of gravel (much higher permeability than sand). A constant flow rate was applied through the bottom (gravel) by a peristaltic pump (Figure 4.4), therefore a constant head difference between top and bottom induced vertical flow. Finally, the head loss was measured and the flow rate at the outflow was recorded. For the three scenarios, the vertical conductivities were obtained with Equation 4-4 and the results are summarized in Table 4.4 through Table 4.6.

$$k_v = \frac{QL}{A\Delta\varphi} \tag{4-4}$$

where, k_v = vertical conductivity (L/T), A = cross sectional area of the sample (L^2), and $\Delta\varphi$ = total head difference across sand column (L).
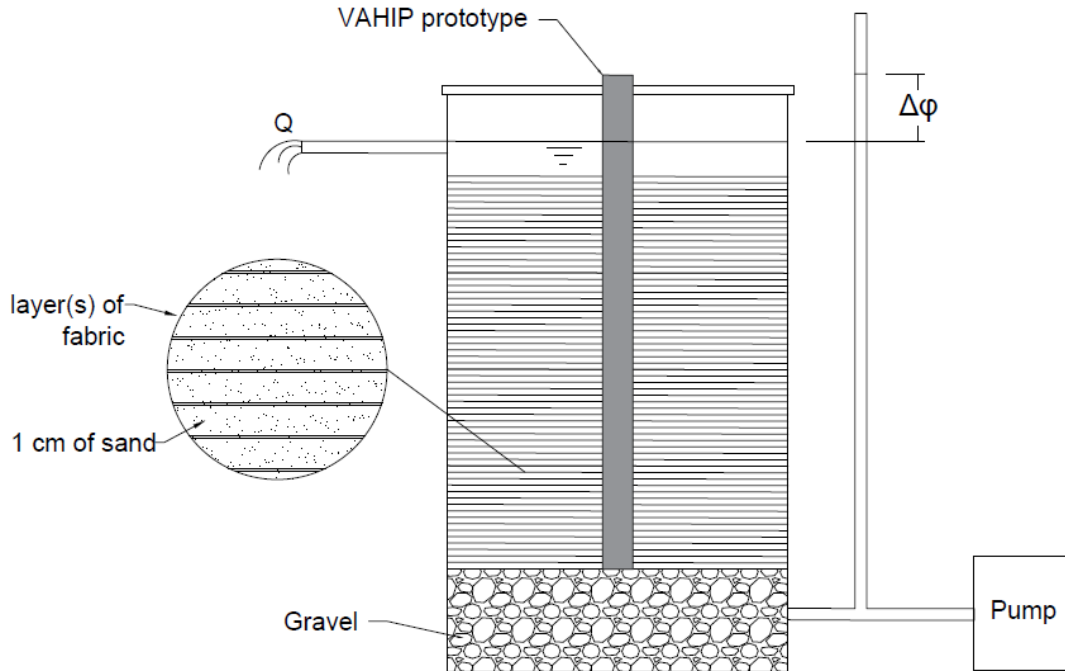
Figure 4.4 Vertical permeability test setup. The VAHIP prototype was only used for injection tests described in following section.

Table 4.4 Vertical conductivity results for the scenario 1, L= 69 cm and A= 2,400 cm^2

Δφ (cm)	Q (cm^3/s)	k$_v$ (cm/s)	k$_{v, average}$ (cm/s)
16.00	14.53	0.026	0.025
11.00	9.16	0.024	
10.30	9.07	0.025	
7.95	7.24	0.026	
6.10	5.46	0.026	
4.30	3.97	0.027	
3.30	2.90	0.025	
2.60	2.14	0.024	
1.55	1.27	0.024	

Table 4.5 Vertical conductivity results for scenario 2 (64 layers of fabric and 65 layers of sand), L= 68.52 cm and A=2,400 cm2

Δφ (cm)	Q (cm³/s)	k_v (cm/s)	$k_{v, average}$ (cm/s)
8.40	5.30	0.018	0.018
7.60	5.00	0.019	
7.00	4.64	0.019	
6.40	4.24	0.019	
5.85	3.82	0.019	
5.10	3.36	0.019	
4.50	2.87	0.018	
3.88	2.39	0.018	
3.35	2.01	0.017	
2.75	1.68	0.017	
2.05	1.11	0.016	
1.30	0.79	0.017	
0.80	0.46	0.016	
7.00	4.64	0.019	

Table 4.6 Vertical conductivity results for scenario 3 (128 layers of fabric and 65 layers of sand), L= 72.04 cm and A=2,400 cm^2

Δφ (cm)	Q (cm³/s)	k_v (cm/s)	$k_{v, average}$ (cm/s)
37.15	16.73	0.014	0.015
32.45	15.36	0.014	
27.50	13.14	0.014	
23.60	11.46	0.015	
19.50	9.29	0.014	
15.40	6.97	0.014	
11.50	5.46	0.014	
8.75	4.26	0.015	
7.70	3.60	0.014	
6.50	3.03	0.014	
4.65	2.27	0.015	
3.15	1.70	0.016	
1.80	1.00	0.017	

Moreover, the flow rate was plotted against AΔφ/L (Figure 4.5) for the three scenarios, where the slope of each trendline corresponds to the vertical conductivity obtained using a linear regression. The R^2 coefficients are close to one for the three trendlines.
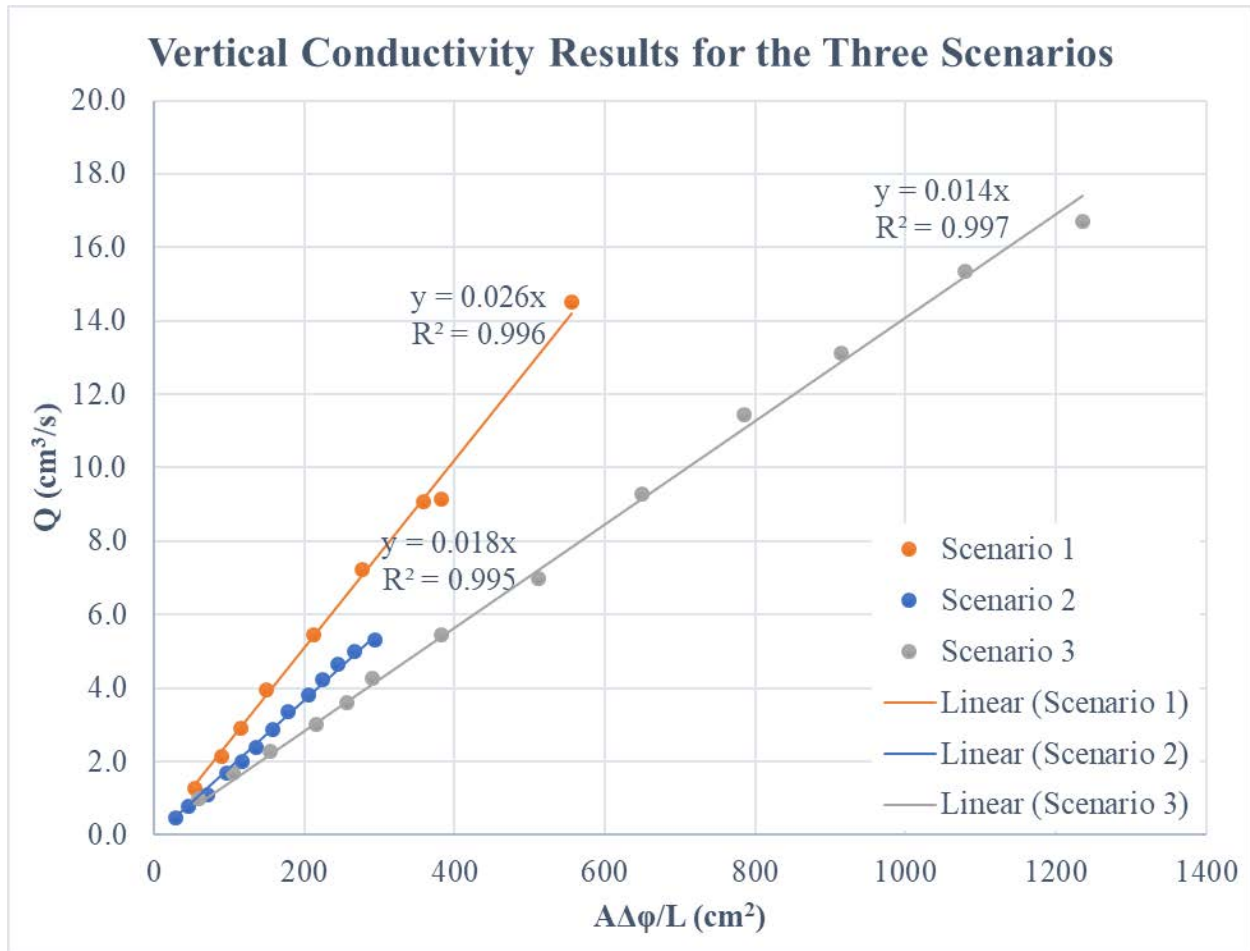
Figure 4.5 Flow rate as a function of AΔh/L for the three anisotropy scenarios

4.5   SAND BARREL INJECTION TEST USING VAHIP PROTOTYPE

The PVC prototype was tested in the same setup where independent vertical flow tests were performed. Before packing the material inside the barrel, the probe was placed at the center and fixed at the top by bolts to avoid lateral movements. The gravel was hydraulically connected to the free-standing water on top of the sand (Figure 4.7). A commercial power supply and three voltmeters (Figure 4.6) were used to record the readings from the pressure transducers. While performing injection tests, the procedure was modified to account for encountered issues, for example, leaking connections between hose and probe. The optimized testing procedure is detailed below.

4.5.1   INJECTION TEST PROCEDURE

1. The readings from the three transducers inside the probe and out of water were recorded.

2. The probe was centered inside the barrel (on top of gravel as shown in Figure 4.7), and the elevation head for each transducer was measured from the barrel bottom to the transducers tip.
3. The sand was wet-packed inside the barrel, which allowed the bottom and middle chambers to be filled. For the layering scenarios, each layer of sand was leveled before placing the fabric.
4. The top chamber was filled with water (this chamber was not completely filled after packing the sand because the probe extended beyond the barrel) to get rid of air that could affect the readings. Then, a hose was connected to the top of the probe.
5. The initial readings before injection were recorded along with the water level inside the barrel.
6. Water was injected through the probe top using a peristaltic pump to provide a constant flow rate (Figure 4.8).
7. Readings during injection were taken once they were stable (steady-state condition), followed by the measurement of the water level inside the barrel.
8. The flow rate at the outflow was recorded.
9. The injection was stopped, allowing the readings to reach static steady-state condition. Steps 5 through 8 were repeated by applying different flow rates.
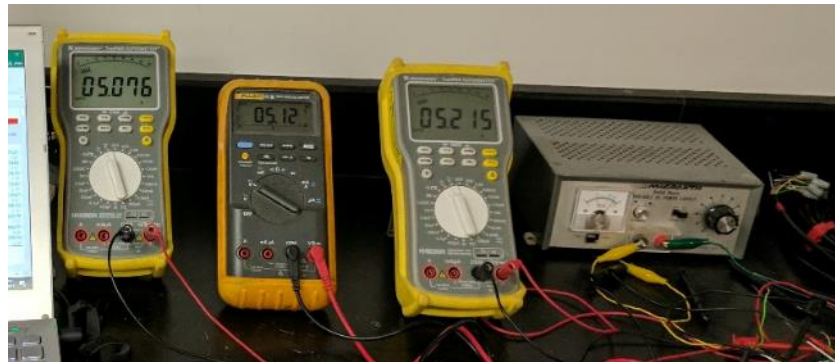
Figure 4.6 Voltmeters and power supply used for the injection tests
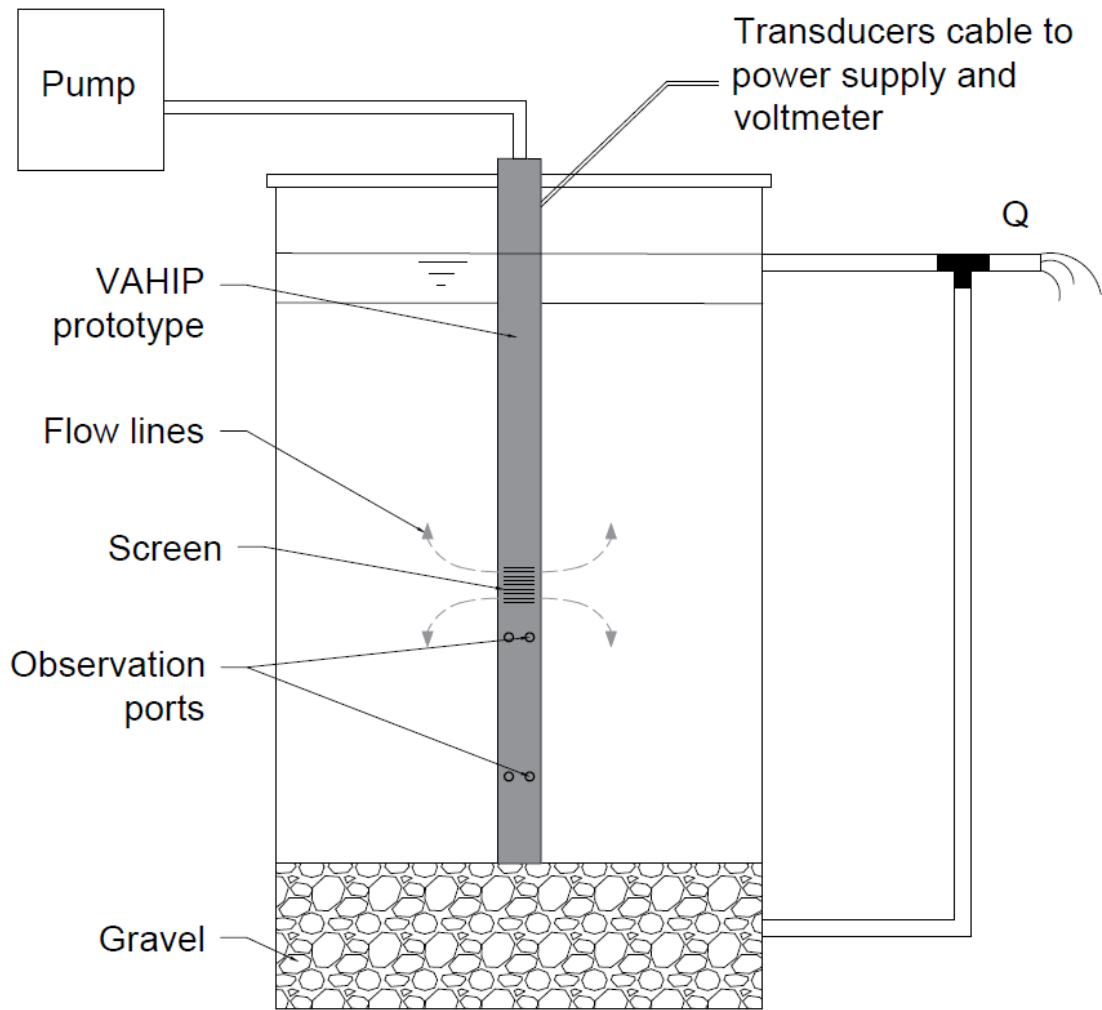
Figure 4.7 Injection test setup using the VAHIP prototype

Figure 4.8 Injection test using the PVC prototype

4.5.2   DATA ANALYSIS

In order to assess vertical and horizontal permeability, a spreadsheet with the data recorded during the injection test was used and analyzed as follows.

1.   The voltage readings before (V_{bi}) and during injection (V_{di}) were converted to pressure heads h_{pbi} (cm) and h_{pdi} (cm), respectively.

$$h_{pbi} = 210.9 \times V_{bi} \tag{4-5}$$

$$h_{pdi} = 210.9 \times V_{di} \tag{4-6}$$

2.   The total head before injection φ_{bi} (cm) was obtained by adding the pressure head and the elevation head h_e (cm) for each transducer.

$$\varphi_{bi} = h_{pbi} + h_e \tag{4-7}$$

3.   The pressure head during injection was added to the elevation head to obtain the total head during injection φ_{di} (cm).

$$\varphi_{di} = h_{pdi} + h_e \tag{4-8}$$

4. To calculate the heads (cm) caused solely by injection (top transducer φ_0, middle transducer φ_{t1}, and bottom transducer φ_{t2}), the heads before injection were subtracted from the heads during injection. It can be noted that the elevation head cancels each other. Moreover, if the water level changed before and during injection that difference Δ (cm) was also subtracted.

$$\varphi_0, \varphi_{t1}, \varphi_{t2} = \varphi_{di} - \varphi_{bi} - \Delta \qquad (4\text{-}9)$$

$$\varphi_0, \varphi_{t1}, \varphi_{t2} = h_{pdi} + h_e - \left(h_{pbi} + h_e\right) - \Delta \qquad (4\text{-}10)$$

$$\varphi_0, \varphi_{t1}, \varphi_{t2} = 210.9(V_{di} - V_{bi}) - \Delta \qquad (4\text{-}11)$$

5. The head ratios φ_{t1}/φ_0, φ_{t2}/φ_0, and $\varphi_{t2}/\varphi_{t1}$ were calculated.

4.5.3 ASSESSMENT OF HORIZONTAL AND VERTICAL CONDUCTIVITY

In order to estimate permeability components using Klammler et al.'s (2011) semi-analytical method, the internal (along probe) and external (barrel) boundaries need to be considered. For the three scenarios, the top and bottom boundaries were set as constant head and the lateral boundary was set as impermeable. The probe casing was considered impermeable except for the injection screen, which was set as a constant head. The test geometry is listed below and depicted in Figure 4.9.

- Probe radius a = 2.1 cm
- Horizontal distance to lateral boundary (barrel radius) b = 27.7 cm
- Screen length s = 4 cm
- Distance from the screen end to the near and far observation port t_1 = 4 cm and t_2 = 20 cm respectively
- Vertical distance from bottom boundary to the screen edge h1 = 30 cm
- The distance between top and bottom boundaries, d, was slightly different for the three scenarios. For scenario 1, d = 69 cm; for scenario 2, d = 68.52 cm; and for scenario 3, d = 72.04 cm.
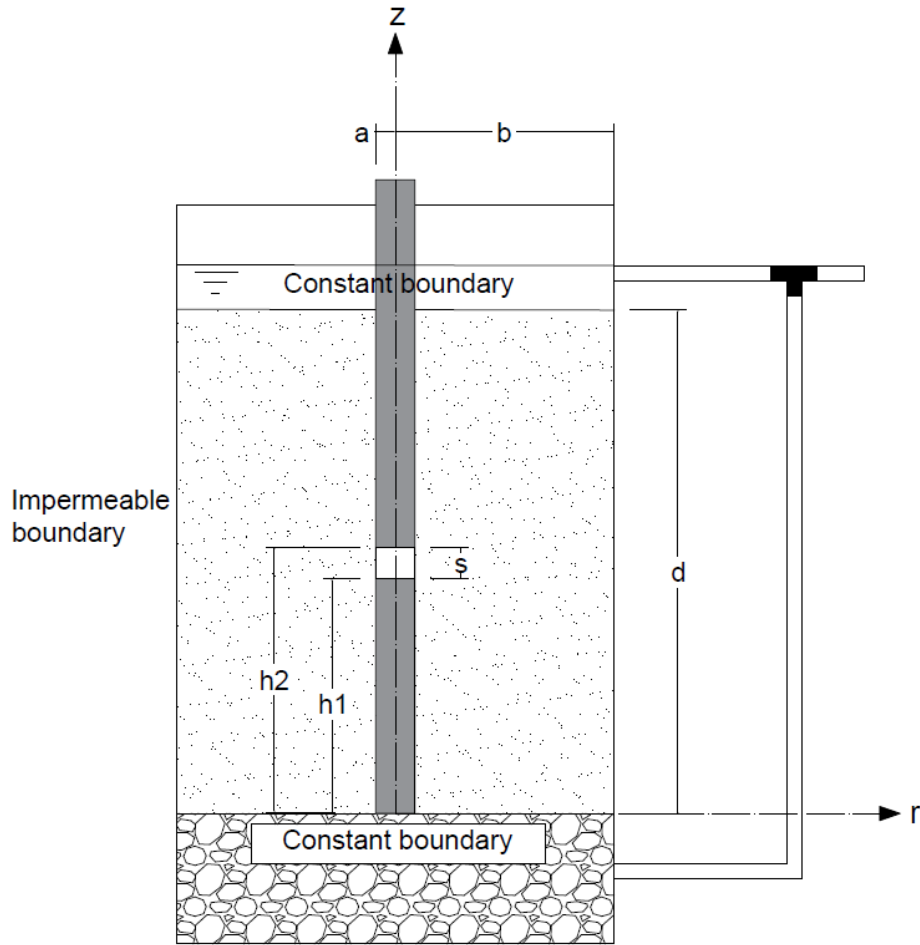
Figure 4.9 Test geometry and external boundary conditions

Dimensionless charts were generated with Matlab where three curves that correspond to the three head ratios previously calculated are shown in Figure 4.10. From this chart, $\log_{10}(s/a\rho)$ is obtained, resulting in the assessment of ρ due to prior knowledge of screen length and probe radius. Subsequently, from Figure 4.11 the shape factor F is obtained. The latter along with the flow rate Q and injection head φ_0 (previously measured) allowed the assessment of the horizontal conductivity through Equation 4-12. Finally, the vertical conductivity is obtained by means of Equation 4-13.
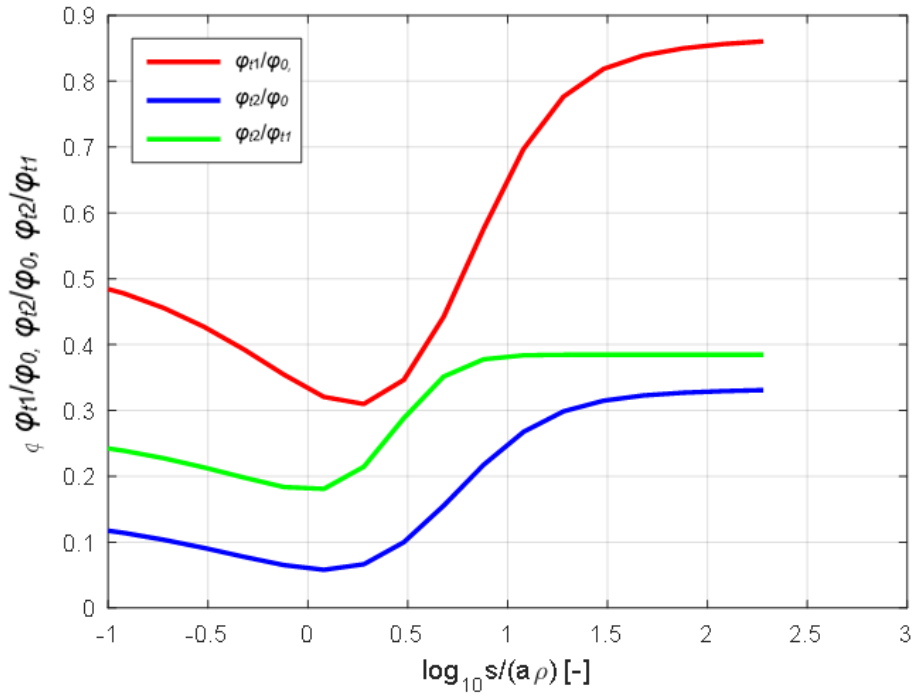
Figure 4.10 Head ratios φt1/φ0, φt2/φ0, and φt2/φt1 as a function of log10(s/aρ) for the specified barrel test geometry
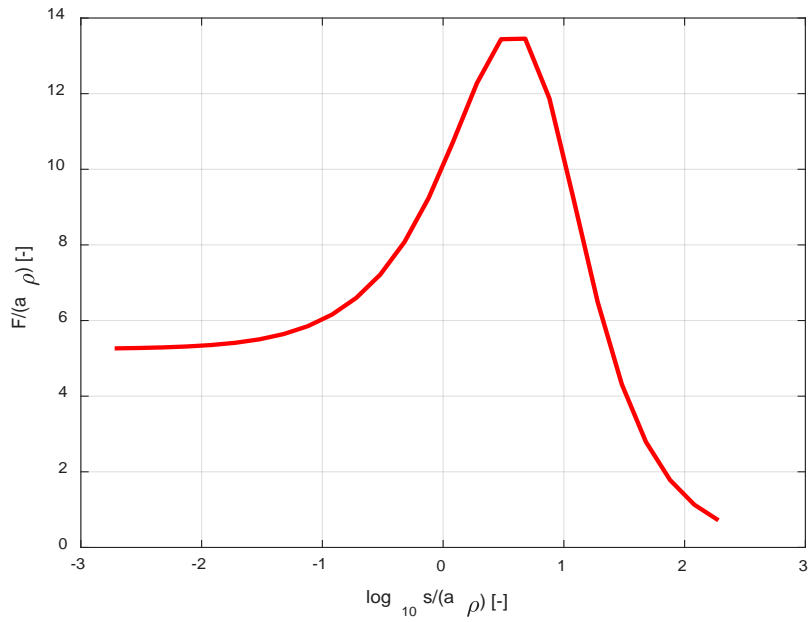
Figure 4.11 F/aρ as a function of log10(s/aρ) for the specified barrel test geometry

$$k_h = \frac{Q}{\varphi_0 F} \tag{4-12}$$

$$k_v = k_h \rho^2 \tag{4-13}$$

4.5.4 INJECTION TEST RESULTS

For the injection tests, different flow rates were applied for each of the three scenarios. As shown in Figure 4.10, three potential estimates of horizontal and vertical conductivity can be obtained from the red φ_{t1}/φ_0, blue φ_{t2}/φ_0, and green $\varphi_{t2}/\varphi_{t1}$ curves.

For laboratory tests where a lateral impermeable boundary is relatively near the probe, some of the head ratios intercept the curves at two different points, meaning that there are two possible solutions for ρ. Therefore, for the case of isotropy where $\rho^2=1$, the abscissa $\log_{10}(s/a\rho)$ has a value of 0.28. Hence, values smaller than 0.28 are for cases where the vertical permeability exceeds the horizontal permeability. Values greater than 0.28 are for anisotropy cases where the horizontal permeability is greater. Based on the preliminary tests, the latter, solution as expected, thus focusing the results on the right side of the curves from $\log_{10}(s/a\rho) = 0.28$.

4.5.4.1 SCENARIO 1 (NO LAYERING)

The horizontal and vertical conductivity results are presented in Table 4.7. For the horizontal results, in most of the measurements, the highest estimates are obtained through the ratio φ_{t1}/φ_0, where an average of $k_h = 0.078$ cm/s was obtained, followed by the ratio φ_{t2}/φ_0 with an average of $k_h = 0.059$ cm/s, and lastly $\varphi_{t2}/\varphi_{t1}$ with an average of $k_h = 0.053$ cm/s. This trend might be a result of the small head measured at the bottom transducer (φ_{t2}) and induced by injection because this is the farthest transducer with respect to the screen. As previously mentioned, the highest k_h correspond to the ratio φ_{t1}/φ_0 that does not depend on φ_{t2}. On the other hand, the lowest estimates are obtained by the ratio $\varphi_{t2}/\varphi_{t1}$, and by having a reduced magnitude of φ_{t2} as the numerator. This will result in a smaller estimate of horizontal conductivity. Moreover, an average horizontal conductivity of $k_h = 0.065$ cm/s from the 18 estimates was computed along with a standard deviation of 0.022 cm/s. The latter compared well to $k_h = 0.069$ cm/s, obtained from constant head tests using horizontal flow in a rectangular box (see section 4.3). For the single estimates (rather than an average), just one value is one order of magnitude greater than the value obtained with the independent horizontal flow test. However, when the three estimates from a single injection test are averaged, the result lies within the same order of magnitude.

Some head ratios do not intersect the corresponding curve, which is expressed as not applicable (N/A). For example, for the first and second injection tests the values of $\varphi t1$ were the same (4.22 cm) for a flow rate of 8.83 and 9.17 cm^3/s (0.34 cm^3/s difference). For the last injection test, a flow rate of 8.41 cm^3/s induced $\varphi_{t1} = 2.11$ cm, which is half the head measured in the first injection test, with a similar Q (0.42 cm^3/s difference). This resulted in a low ratio, $\varphi_{t1}/\varphi_0 = 0.29$, that did not intersect the corresponding curve. Another example is the sixth injection test with the highest Q (16.15 cm^3/s), where the induced head φ_{t2} was not the highest, thus the ratio $\varphi_{t2}/\varphi_{t1}$ was too small

31

to provide estimates of conductivity. The N/A cells might have been a result of unknown errors and the lower resolution (2.1 cm) for the middle transducer.

The opposite happened with the vertical component, in which the lowest estimate was obtained by means of the φ_{t1}/φ_0 curve, corresponding to an average $k_v = 0.015$ cm/s, followed by $k_v = 0.024$ cm/s, and lastly the highest average $k_v = 0.028$ cm/s. An overall average $k_v = 0.022$ cm/s agrees well with $k_v = 0.025$ cm/s, which is the average obtained from the vertical flow constant head test in the same setup where the injection test was performed (see section 4.4). Moreover, all estimates of vertical conductivity are in the same order of magnitude with a standard deviation of 0.0092 cm/s.

Table 4.7 Conductivity results from injection test for scenario 1

φ_0 (cm)	φ_{t1} (cm)	φ_{t2} (cm)	φ_{t1}/φ_0	φ_{t2}/φ_0	$\varphi_{t2}/\varphi_{t1}$	Q (cm^3/s)	Log$_{10}$ (s/aρ)	Log$_{10}$ (s/aρ)	Log$_{10}$ (s/aρ)
9.70	4.22	0.84	0.44	0.087	0.20	8.83	0.66	0.40	0.19
11.18	4.22	0.63	0.38	0.057	0.15	9.17	0.54	N/A	N/A
12.02	6.33	2.11	0.53	0.18	0.33	11.05	0.80	0.74	0.61
13.92	6.33	1.69	0.46	0.12	0.27	12.97	0.67	0.55	0.41
15.85	5.73	1.51	0.36	0.095	0.26	15.46	0.51	0.45	0.41
17.08	7.38	1.05	0.43	0.062	0.14	16.15	0.66	N/A	N/A
10.03	3.92	0.75	0.39	0.075	0.19	9.83	0.57	0.33	N/A
7.38	2.11	0.63	0.29	0.086	0.30	8.41	N/A	0.39	0.51

Note: the red, blue, and green values for log$_{10}$(s/aρ) are the obtained through the red, blue, and green curves in Figure 4.10 respectively.

Table 4.7 Conductivity results from injection test for scenario 1 - Continued

F/aρ	F/aρ	F/aρ	k_h (cm/s)	k_h (cm/s)	k_h (cm/s)	k_v (cm/s)	k_v (cm/s)	k_v (cm/s)
13.34	12.89	11.52	0.078	0.044	0.031	0.014	0.026	0.046
13.34	N/A	N/A	0.053	N/A	N/A	0.016	N/A	N/A
12.36	12.84	13.34	0.12	0.099	0.070	0.011	0.012	0.015
13.21	13.34	12.98	0.088	0.063	0.047	0.013	0.018	0.025
13.35	13.17	12.92	0.059	0.052	0.048	0.021	0.024	0.027
13.34	N/A	N/A	0.080	N/A	N/A	0.014	N/A	N/A
13.34	12.49	N/A	0.068	0.042	N/A	0.018	0.033	N/A
N/A	12.85	13.65	N/A	0.055	0.069	N/A	0.033	0.024
		Average	0.078	0.059	0.053	0.015	0.024	0.028
		Average	0.065			0.022		

Note: the red, blue, and green values for F/aρ, k_h, and k_v are the obtained through the red, blue, and green curves in Figure 4.10 respectively.

The heads were plotted against the flow rate (Figure 4.12) and a linear regression was used. The interception was set to zero as zero flow rate corresponds to zero head due to injection. The slope of each trendline was used to calculate the head ratios to enter the charts, consequently, obtaining three potential estimates of conductivity as shown in Table 4.8.
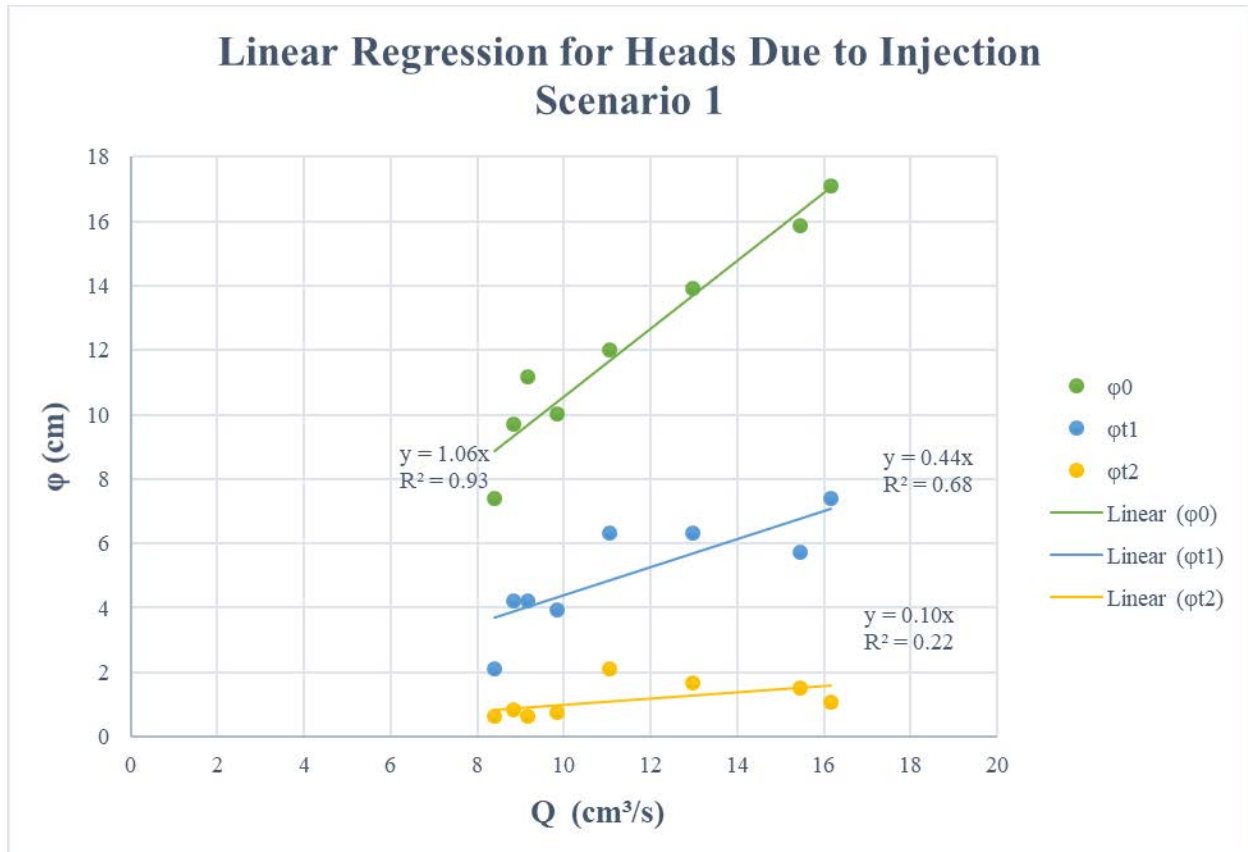
Figure 4.12 Injection test, scenario 1 linear trendline for heads φ0, φt1, and φt2

From Figure 4.12 it can be observed that the coefficient of determination (R^2=0.22) for φ_{t2} is not as good as for the other two heads. The small pressures measured at the bottom transducer (farthest transducer from the injection screen) and the error of ±2.1 cm associated with the measurements might have impacted the coefficient of determination. Thus, if only the estimates of conductivity k_h= 0.074 cm/s (compared to 0.069 cm/s), and k_v= 0.015 cm/s (compared to 0.025 cm/s) from the φ_{t1}/φ_0 ratio are considered, the estimates are also very close to the independent horizontal and vertical flow tests.

Table 4.8 Horizontal and vertical conductivity values from injection tests using linear regression for the scenario 1

φ_{t1}/φ_0	φ_{t2}/φ_0	$\varphi_{t2}/\varphi_{t1}$	k_h (cm/s)	k_h (cm/s)	k_h (cm/s)	k_v (cm/s)	k_v (cm/s)	k_v (cm/s)
0.42	0.094	0.23	0.074	0.050	0.039	0.015	0.024	0.034
		Average		0.054			0.024	

Note: the red, blue, and green values for or F/aρ, k_h, and k_v are the obtained through the red, blue, and green curves in Figure 4.10 respectively.

33

4.5.4.2 SCENARIO 2

For this test, estimates with the $\varphi_{t2}/\varphi_{t1}$ curve were not possible to obtain since the ratio did not intersect the corresponding curve (Table 4.9). These N/A values might have been caused due to pressures measured by the middle transducer (in Appendix A, Table A-2). It can be seen that four measurements recorded by the middle transducer are the same even though the flow rate varied between 14.52 and 12.62 cm^3/s. Moreover, the second and third N/A entries for the ratio φ_{t1}/φ_0 (red), resulted due to the higher injection heads that are not in accordance (three times larger) with similar flow rates (e.g., sixth injection test). For the horizontal hydraulic conductivity permeability, an average equal to $k_h = 0.2115$ cm/s from the nine estimates was obtained along with a standard deviation of 0.01406 cm/s, while for the independent conductivity measurements using a constant head test had an average of $k_h = 0.14386$ cm/s. Both values compared well, although estimates from two individual tests were one order of magnitude smaller.

From the injection test, an average $k_v = 0.018$ cm/s was obtained. On the other hand, the same value $k_v = 0.018$ cm/s was obtained as an average from the independent vertical flow test, resulting in the closest estimates. Additionally, all individual estimates ranged within the same order of magnitude with a standard deviation of 0.0068 cm/s.

Table 4.9 Conductivity results from injection test for scenario 2

φ_0 (cm)	φ_{t1} (cm)	φ_{t2} (cm)	φ_{t1}/φ_0	φ_{t2}/φ_0	$\varphi_{t2}/\varphi_{t1}$	Q (cm^3/s)	Log$_{10}$ (s/aρ)	Log$_{10}$ (s/aρ)	Log$_{10}$ (s/aρ)
10.41	15.47	2.61	1.49	0.25	0.17	17.99	N/A	1.01	N/A
23.66	3.42	2.15	0.14	0.091	0.63	14.52	N/A	0.42	N/A
32.56	3.25	1.98	0.10	0.061	0.61	13.31	N/A	N/A	N/A
6.35	1.71	1.29	0.27	0.20	0.75	9.40	N/A	0.83	N/A
11.54	5.43	2.69	0.47	0.23	0.50	17.10	0.72	0.94	N/A
10.48	3.52	2.25	0.34	0.22	0.64	13.50	0.42	0.87	N/A
8.47	3.62	2.14	0.43	0.25	0.59	12.62	0.65	1.02	N/A

Note: the red, blue, and green values for log$_{10}$(s/aρ) are the obtained through the red, blue, and green curves in Figure 4.10 respectively.

Table 4.9 Conductivity results from injection test for scenario 2 - Continued

F/aρ	F/aρ	F/aρ	k_h (cm/s)	k_h (cm/s)	k_h (cm/s)	k_v (cm/s)	k_v (cm/s)	k_v (cm/s)
N/A	10.03	N/A	N/A	0.44	N/A	N/A	0.015	N/A
N/A	13.03	N/A	N/A	0.031	N/A	N/A	0.016	N/A
N/A	N/A	N/A	N/A	N/A	N/A	N/A	N/A	N/A
N/A	12.14	N/A	N/A	0.21	N/A	N/A	0.016	N/A
13.02	10.98	N/A	0.15	0.29	N/A	0.020	0.014	N/A
12.99	11.83	N/A	0.065	0.20	N/A	0.035	0.013	N/A
13.34	9.90	N/A	0.12	0.39	N/A	0.023	0.013	N/A
		Average	0.11	0.26	N/A	0.026	0.015	N/A
		Average	0.21			0.018		

Note: the red, blue, and green values for F/aρ, k_h, and k_v are the obtained through the red, blue, and green curves in Figure 4.10 respectively.

The heads were plotted in Figure 4.13, showing low R^2 values for φ_0 and φ_{t1}. By visual inspection, three data points corresponding to the highest heads were found to be suspicious and excluded as potential outliers due to unknown errors. The linear trendlines without the outliers can be seen in Figure 4.14. The components of hydraulic conductivity obtained using a linear regression without the possible outliers were k_h = 0.19 cm/s (compared with 0.14 cm/s) and k_v = 0.019 cm/s (compared with 0.018 cm/s), and are presented in Table 4.10.
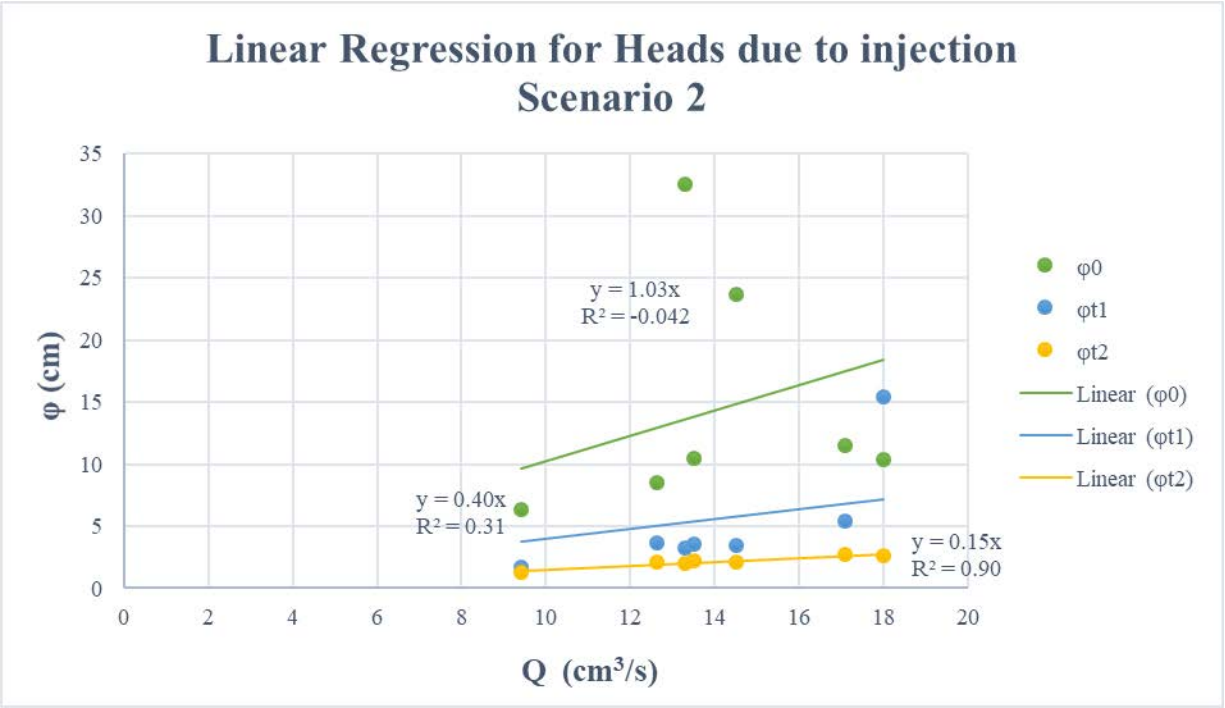
Figure 4.13 Injection test for scenario 2 linear trendline for heads φ0, φt1, and φt2

Figure 4.14 Injection test for scenario 2 linear trendline for heads φ0, φt1, and φt2, without possible outliers

Both estimates obtained with and without the possible outliers compared very well to those obtained by independent horizontal and vertical flow tests, thus the outliers do not represent a significant impact on the estimates.

Table 4.10 Horizontal and vertical conductivity values for injection tests using linear regression for scenario 2 (without possible outliers).

φ_{t1}/φ_0	φ_{t2}/φ_0	$\varphi_{t2}/\varphi_{t1}$	k_h (cm/s)	k_h (cm/s)	k_h (cm/s)	k_v (cm/s)	k_v (cm/s)	k_v (cm/s)
0.40	0.23	0.57	0.10	0.27	N/A	0.025	0.014	N/A
		Average		0.19			0.019	

Note: the red, blue, and green values for or F/aρ, k_h, and k_v are the obtained through the red, blue, and green curves in Figure 4.10 respectively.

4.5.4.3 SCENARIO 3

Six injection tests were performed in this scenario (Table 4.11), where twelve estimates of conductivity were obtained and when averaged, the horizontal conductivity was $k_h = 0.20$ cm/s, which compared well with $k_h = 0.17$ cm/s obtained from the horizontal flow measurements using a constant head test. A standard deviation of 0.19 cm/s was computed from the twelve estimates, where three of them were one order of magnitude less than those obtained through an independent horizontal flow test. When the three estimates obtained for a single injection test were averaged, the results were in the same order of magnitude and compared well.

Additionally, an average $k_v = 0.017$ cm/s was estimated and compared well to $k_v = 0.015$ cm/s obtained by means of independent vertical flow tests. Moreover, a standard deviation of 0.0075 cm/s was computed. It can be observed that one of the vertical conductivity values is one order of magnitude smaller than the rest; however, when the three estimates are averaged, the resultant shows good agreement with $k_v = 0.015$ cm/s.

In Table 4.11 there is a negative head φ_{t2}, which is due to the fact that the measured head during injection was smaller than the measured head before injection as presented in Table A-3, thus, resulting in N/A cells. Additionally, for the last two injection tests, the difference between the pressure head before and after injection is minimal (Table A-3), resulting in low observation heads at the bottom transducer that translated in low head ratios to intersect each curve.

Table 4.11 Conductivity results from injection test for scenario 3

φ_0 (cm)	φ_{t1} (cm)	φ_{t2} (cm)	φ_{t1}/φ_0	φ_{t2}/φ_0	$\varphi_{t2}/\varphi_{t1}$	Q (cm³/s)	Log₁₀ (s/aρ)	Log₁₀ (s/aρ)	Log₁₀ (s/aρ)
14.26	8.99	2.87	0.63	0.20	0.32	15.09	0.97	0.83	0.57
11.50	7.28	2.01	0.63	0.18	0.28	13.77	0.97	0.74	0.44
8.54	6.43	1.79	0.75	0.21	0.28	11.32	1.22	0.85	0.45
5.05	2.31	-0.01	0.46	-0.002	-0.005	6.44	0.70	N/A	N/A
4.00	2.31	0.20	0.58	0.050	0.087	4.74	0.88	N/A	N/A
8.49	4.27	0.26	0.50	0.031	0.061	10.13	0.77	N/A	N/A

Note: the red, blue, and green values for $\log_{10}(s/a\rho)$ are the obtained through the red, blue, and green curves in Figure 4.10 respectively.

Table 4.11 Conductivity results from injection test for scenario 3 - Continued

F/aρ	F/aρ	F/aρ	k_h (cm/s)	k_h (cm/s)	k_h (cm/s)	k_v (cm/s)	k_v (cm/s)	k_v (cm/s)
10.59	12.17	13.34	0.23	0.15	0.073	0.0098	0.012	0.020
10.52	12.86	13.13	0.27	0.13	0.063	0.011	0.015	0.030
7.23	11.97	13.16	0.76	0.20	0.071	0.010	0.014	0.033
13.18	N/A	N/A	0.12	N/A	N/A	0.018	N/A	N/A
11.73	N/A	N/A	0.19	N/A	N/A	0.012	N/A	N/A
12.63	N/A	N/A	0.14	N/A	N/A	0.015	N/A	N/A
		Average	0.29	0.16	0.069	0.012	0.014	0.027
		Average	0.20			0.015		

Note: the red, blue, and green values for F/aρ, k_h, and k_v are the obtained through the red, blue, and green curves in Figure 4.10 respectively.

When linear regressions were performed for the three heads, the coefficients of determination R^2 were better in general (Figure 4.15) compared to scenarios 1 and 2 described above. This improvement might have been due to slight modifications made to these injection tests (scenario 3 was the last test performed). Such modifications were: (1) the distance between the rubber stoppers and the observation ports was minimized to reduce the air in the system, (2) small gaps between the stoppers and pressure transducers were sealed with silicone to better isolate chambers, and (3) for the middle and bottom transducer, the tip was placed below the observation port. In previous tests, the level of the transducer tip and the observation ports was the same, and the transducer tip was at the interface between water and air. The average components of conductivity obtained using a linear regression were $k_h = 0.13$ cm/s (compared with 0.17 cm/s) and $k_v = 0.018$ cm/s (compared with 0.015 cm/s), as shown in Table 4.12.

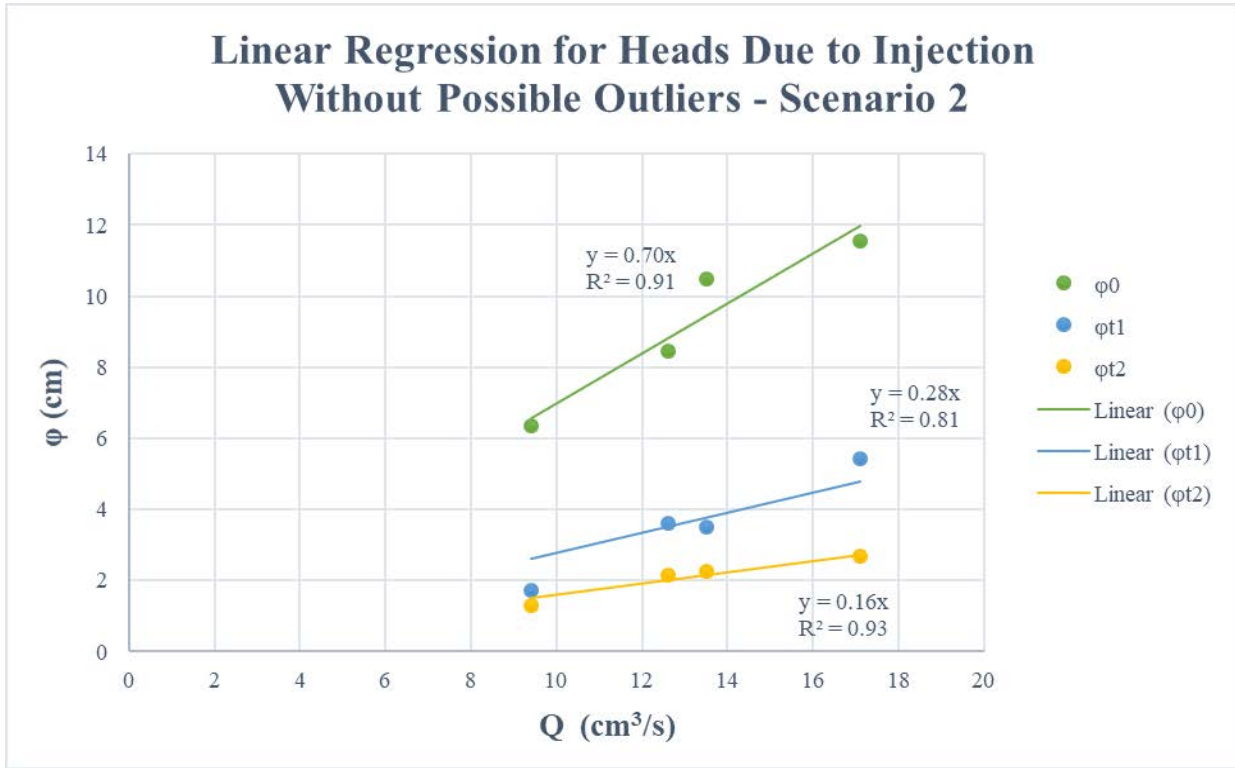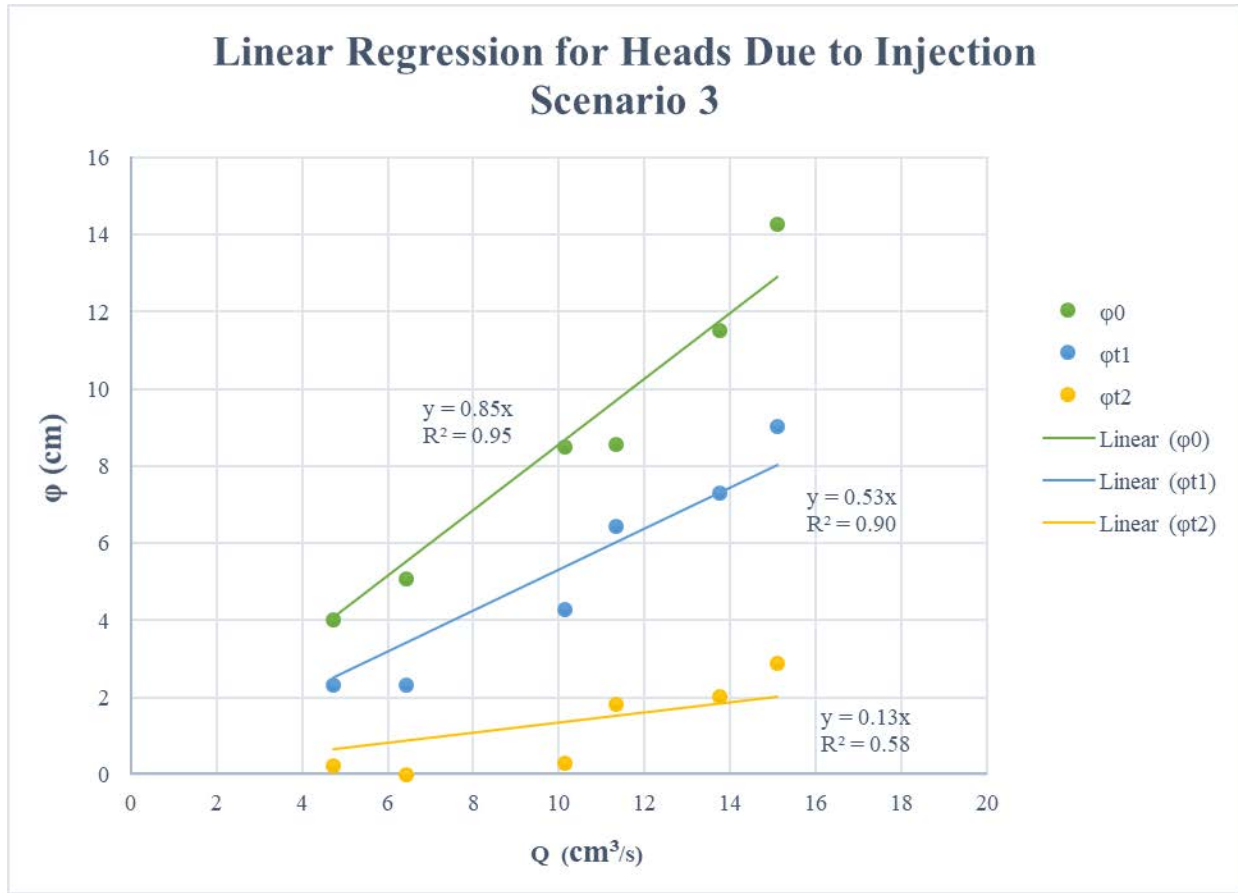Figure 4.15 Injection test for scenario 3 linear trendline for heads φ0, φt1, and φt2

Table 4.12 Horizontal and vertical conductivity values for injection tests using linear regression for the scenario 3

φ_{t1}/φ_0	φ_{t2}/φ_0	$\varphi_{t2}/\varphi_{t1}$	k_h (cm/s)	k_h (cm/s)	k_h (cm/s)	k_v (cm/s)	k_v (cm/s)	k_v (cm/s)
0.62	0.16	0.25	0.24	0.10	0.039	0.011	0.017	0.026
		Average		0.13			0.018	

Note: the red, blue, and green values for or F/aρ, k_h, and k_v are the obtained through the red, blue, and green curves in Figure 4.10 respectively.

39

4.5.5   DISCUSSION

The comparison of both estimates of horizontal and vertical hydraulic conductivity from the VAHIP is good when averaged for a single injection test (Table 4.13). This satisfies field operational criteria of the probe and negates the previous requirement to run multiple injection rates at the same desired depth. All average values of conductivity for one injection rate, except for the first estimate corresponding to the scenario 2, are in the same order of magnitude as the values obtained through independent horizontal and vertical flow using constant head tests. That discrepancy (within one order of magnitude of independent conductivity measurements) might have been due to the fact that scenario 2 was the first series of tests to be performed, and for scenario 3, modifications were made in order to improve the test based on issues found in the previous scenarios. Additionally, only a single estimate was obtained; therefore, it was not possible to calculate an average value. When the heads were plotted against the flow rate, this value appeared to be a possible outlier.

Table 4.13 Summary of horizontal and vertical conductivity from independent tests (horizontal and vertical flow) and injection tests

	Independent horizontal and vertical flow tests			Injection tests		
	k_h (cm/s)	k_v (cm/s)	ρ^2	k_h (cm/s)	k_v (cm/s)	ρ^2
Scenario 1	0.069	0.025	0.360	0.065	0.022	0.330
Scenario 2	0.140	0.018	0.130	0.210	0.018	0.087
Scenario 3	0.170	0.015	0.084	0.200	0.017	0.083

All the vertical conductivity estimates, except for one, are within the same order of magnitude as those obtained through independent vertical flow tests. In most of the injection tests, the highest estimates for the horizontal component was obtained through the φ_{t1}/φ_0 curve, followed by φ_{t2}/φ_0, and lastly $\varphi_{t2}/\varphi_{t1}$. For the vertical conductivity values, an opposite trend occurred.
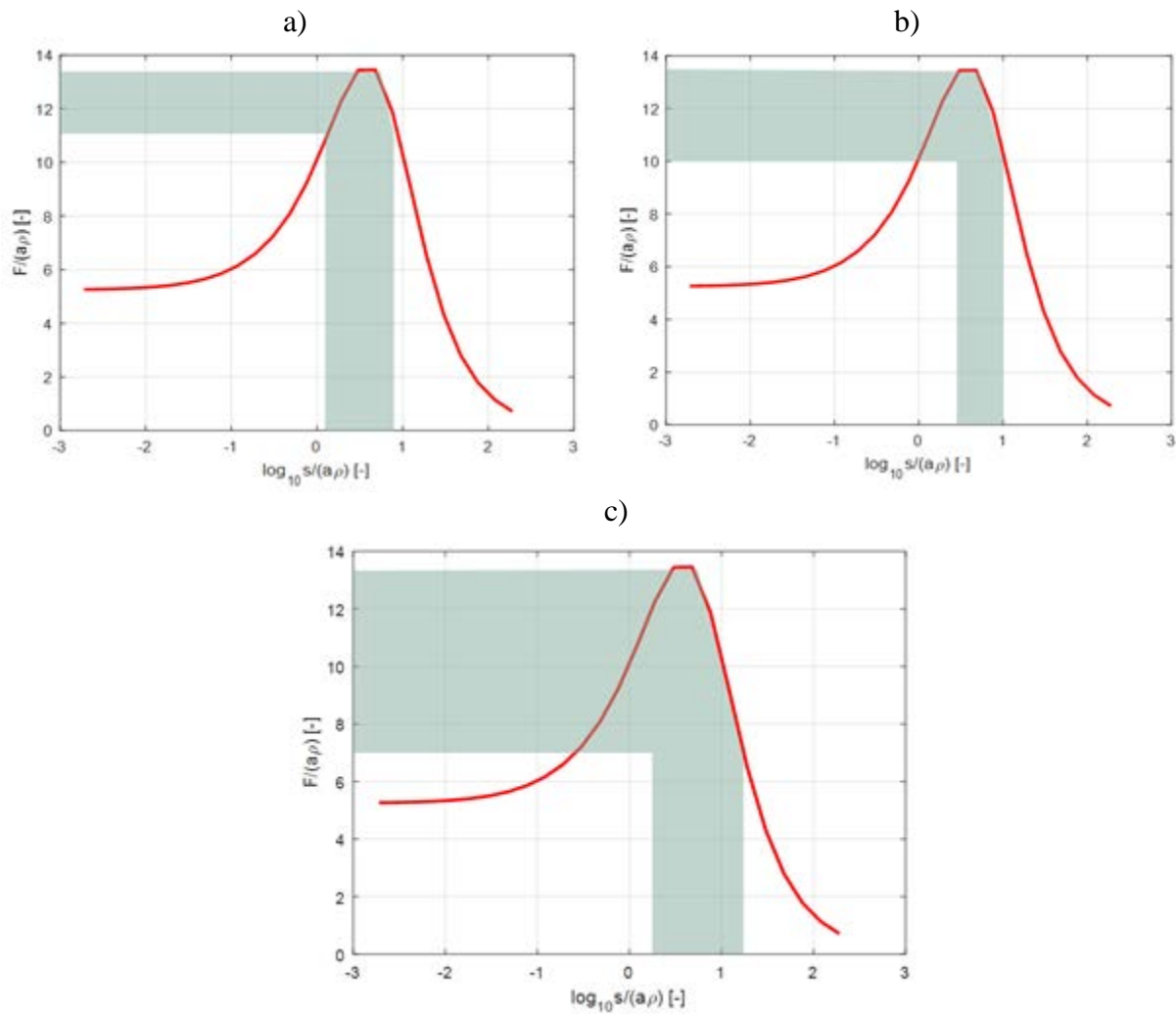
Figure 4.16 Ranges (shaded areas) of anisotropy and shape factor for (a) scenario 1, (b) scenario 2, and (c) scenario 3

The range of anisotropy, and therefore $\log_{10}(s/a\rho)$ (abscissa), and the range of shape factor translated into $F/a\rho$ (ordinate) for the three scenarios is shown in Figure 4.16. Results indicate that scenario 3 presented a wider range in both the abscissa and the ordinate. For scenario 3, the largest estimate of horizontal conductivity was $k_h = 0.76$ cm/s, while the lowest was $k_h = 0.063$ cm/s. The latter is twelve times smaller than the highest estimate, showing that using single estimates rather than an average can lead to less accurate estimates of permeability.

5. PVC-PROTOTYPE TESTING AT FDOT TEST PIT AND RESULTS

Several injection tests were performed in the test pit facility at the Florida Department of Transportation (FDOT) using the Vertical and Horizontal In situ Permeameter (VAHIP) PVC prototype. To run the test, the compaction of the soil took at least two days to prepare. The ground water table was adjusted by raising and lowering it to compact the soil for different time intervals. The compacted and saturated condition of the test pit was used to compare horizontal and vertical permeability.

The objectives of these VAHIP test were:

- Verify the proper performance of the PVC prototype;
- Modify the testing procedures based on issues encountered;
- Verify data transmission, real time visualization, and storage from the PVC prototype readings;
- Analyze data and discuss test results.

5.1   PROCEDURE

1. Lower the water table 30 inches below ground elevation two days prior to testing.
2. The following day, hand auger 27 inches into the soil.
3. Insert probe with an embedment depth of 27 inches.
4. Place soil in the annular space between the probe and the soil.
   a) Use a tamping rod to pack soil within the annular space.
   b) Compact the soil at the surface with a square hand tamper.
5. Level the falling head vessel on the platform.
6. Raise the water level to surface elevation.
7. Drop the water level below the probe tip (27 inches) at the end of the day to allow the soil to naturally consolidate.
8. On the morning of test, raise the water level to the desired test elevation (e.g., six inches below surface). Note: Try to avoid stepping into the test pit as this may disturb the testing environment.
9. Prior to starting the test, drop the water level 6 to 12 inches to create an effluent drainage port. Note: When the water table is not lowered prior to testing, a boundary condition is created, and piping is likely to occur (this occurred multiple times and prevents testing for that day).
10. Follow instructions contained within the VAHIP Labview Program Manual (computer setup shown in Figure 5.1)
    a) Confirm the computer, data acquisition module (DAQ), and sensors are functioning properly. A livestream should be visible on the computer.
    b) After confirmation, the test can be initiated.
11. Start test (a completed set up of the test pit as shown in Figure 5.2).
    a) Fill the falling head vessel with water to the 15-inch mark. Allow water to permeate into the soil.
    b) Remove all air voids within the probe and hose. This will require shaking the hose. Try to avoid entering the test pit area.

> i. Once you believe all of the air voids have been removed, the test can be started.

c) Fill the falling head vessel with water to the 16-inch mark and prepare to start recording when the water level approaches the 15-inch mark.

d) When ready, simultaneously start recording on the computer, start a stop watch, and mark the initial reading on the falling head vessel.

e) Mark a reading on the falling head vessel at every 30 second increment.

f) Conduct the test for 15 minutes.

g) At the conclusion of each test, record all data marked on the falling head vessel and erase the marks. Follow the Labview procedure to save all recorded data from the computer. This will conclude the test.

h) Repeat steps 11.c through 11.g three more times. This will provide a saturation period of 15 minutes from the first test, and the 3 individual, 15-minute tests which will be used for analysis.
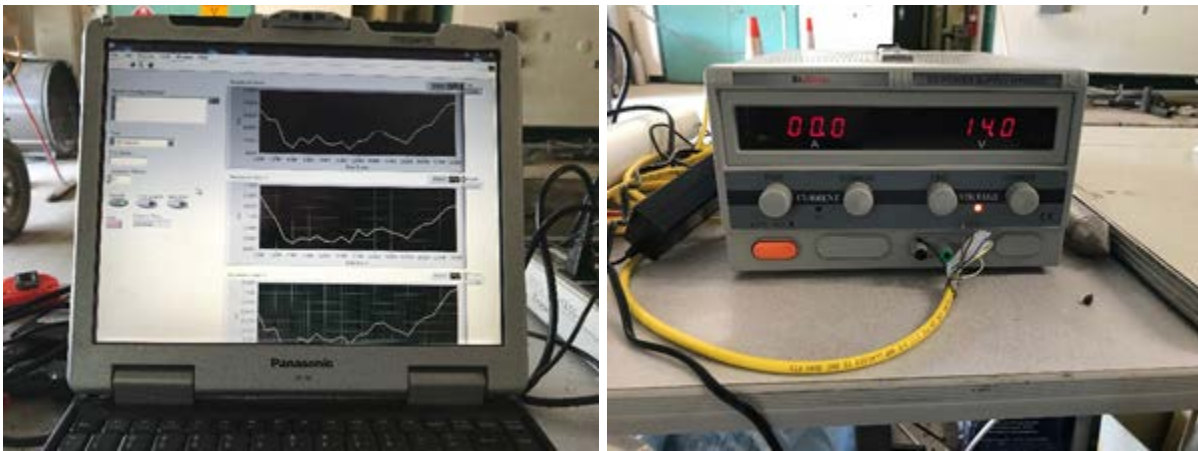
Figure 5.1 VAHIP Labview Program screenshot with power supply used for the FDOT test pit

Figure 5.2   The setup of test pit at the FDOT State Materials Office using the PVC prototype

5.2   DATA ANALYSIS

In order to assess vertical and horizontal permeability, the data recorded during the injection test was analyzed as follows.

1. The average background pressure ($P_{top/0}$, $P_{middle,0}$, $P_{bottom,0}$) was the average pressure of the test pit measured from each transducer (Top, Middle, Bottom) before the injection of water. The measurements of the average background pressure were measured in units of meter of water column, shown in Figure 5.3.

2. The difference between average background pressure and measured pressure from each transducer was found, shown in Figure 5.4:

$$\Delta P_{top} = P_{top} - P_{top,0} \qquad (5\text{-}1a)$$

$$\Delta P_{middile} = P_{middle} - P_{middle,0} \qquad (5\text{-}1b)$$

$$\Delta P_{bottom} = P_{bottom} - P_{bottom,0} \qquad (5\text{-}1c)$$

3. The ratio of the middle transducer to the top transducer and the ratio of bottom transducer to the top transducer were calculated for later use, shown in Figure 5.5:

$$\text{Ratio middle,} R_m = \frac{\Delta P_{middle}}{\Delta P_{top}} \qquad (5\text{-}2a)$$

$$\text{Ratio bottom,} R_b = \frac{\Delta P_{bottom}}{\Delta P_{top}} \qquad (5\text{-}2b)$$

44

4. The flow rate of the water vessel in two-minute intervals are shown in Figure 5.7. The dt was 120 seconds, which was the time interval for the PVC probe to take each reading/measurement:

$$Q = \frac{(\Delta P_{top,t=120s} - \Delta P_{top,t=0s}) \times A_{cross\ section}}{dt} \tag{5-3}$$

5. The anisotropy ratio ρ was found from Figure 5.6; s was the length of the lateral screen; and t_1 was the distance from the lateral screen to the first monitor head. φ_0 is the normalized head, and it is equal to the difference of injection head and background head. Therefore, the φ_0 is same as the pressure difference (ΔP_{top}) of the top transducer.

For $\log_{10}(s/\rho a) > 0.5$:

$$\frac{F}{\rho a} \approx \frac{2\pi \dfrac{s}{\rho a}}{\ln \dfrac{s}{\rho a}} \tag{5-4a}$$

For $-1 < \log_{10}(s/\rho a) < 2$:

$$\frac{F}{\rho a} \approx 9.66[\left(\frac{s}{\rho a}\right)^{0.175}] \tag{5-4b}$$

6. Horizontal conductivity k_h, $Q/\Delta P_{top}$ in two-minute intervals (120 seconds) is shown in Figure 5.6 and the Table 5.2:

$$K_h = \frac{Q}{F \Delta P_{top}} \tag{5-5}$$

7. Vertical conductivity k_v:

$$\rho = \sqrt{\frac{K_v}{K_h}} \tag{5-6}$$

$$K_v = K_h \rho^2$$

5.3   ASSESSMENT OF HORIZONTAL AND VERTICAL CONDUCTIVITY
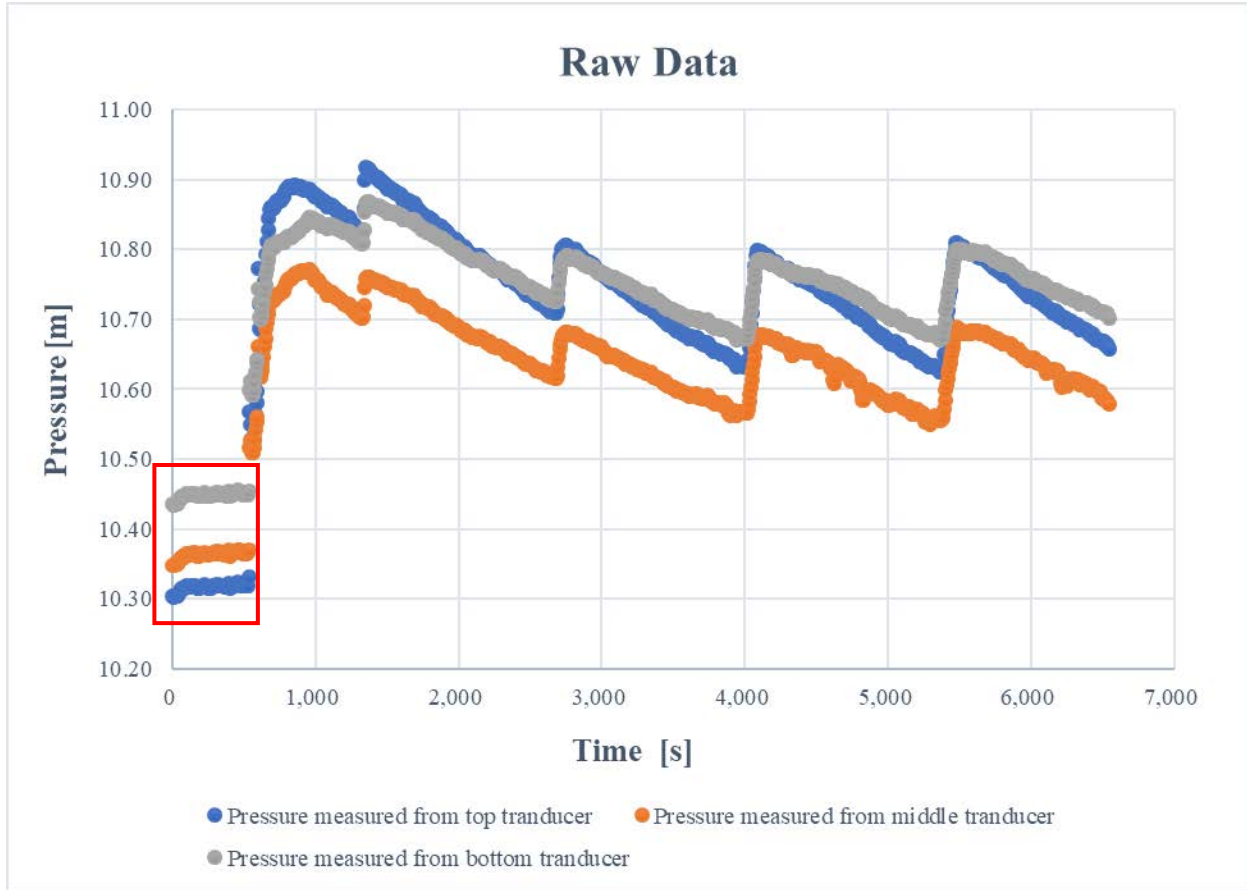
Figure 5.3 The raw data of the test pit had three data sets measured from the top, middle, and bottom transducers. The measurements taken before the injection are shown in the red box. These points were used to find the average background pressure in the test pit.

Table 5.1 The average background pressure of test pit measured from each transducer

$P_{top,0}$ (m)	$P_{middle,0}$ (m)	$P_{bottom,0}$ (m)
10.32	10.37	10.45

The pressures taken from each transducer include atmospheric pressure with the measurements recorded in meters (of water column). Table 5.1 shows the average background pressure taken from each set of data. The average background pressure measured were 10.32 m, 10.37 m, and 10.45 m, from the top, middle, and bottom transducers respectively.
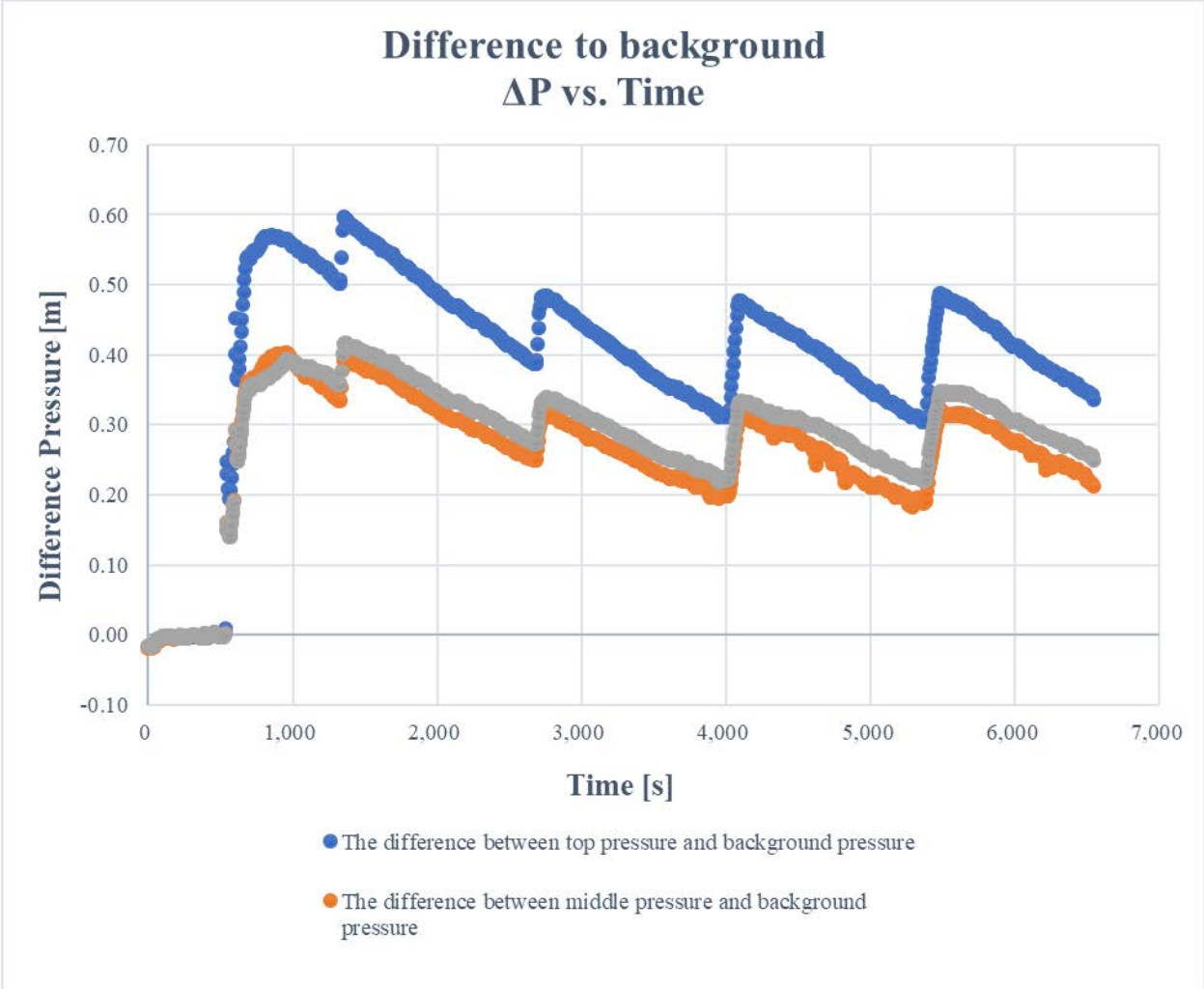
Figure 5.4 The difference between the average background pressure and the pressure
measurements taken from all the transducers.
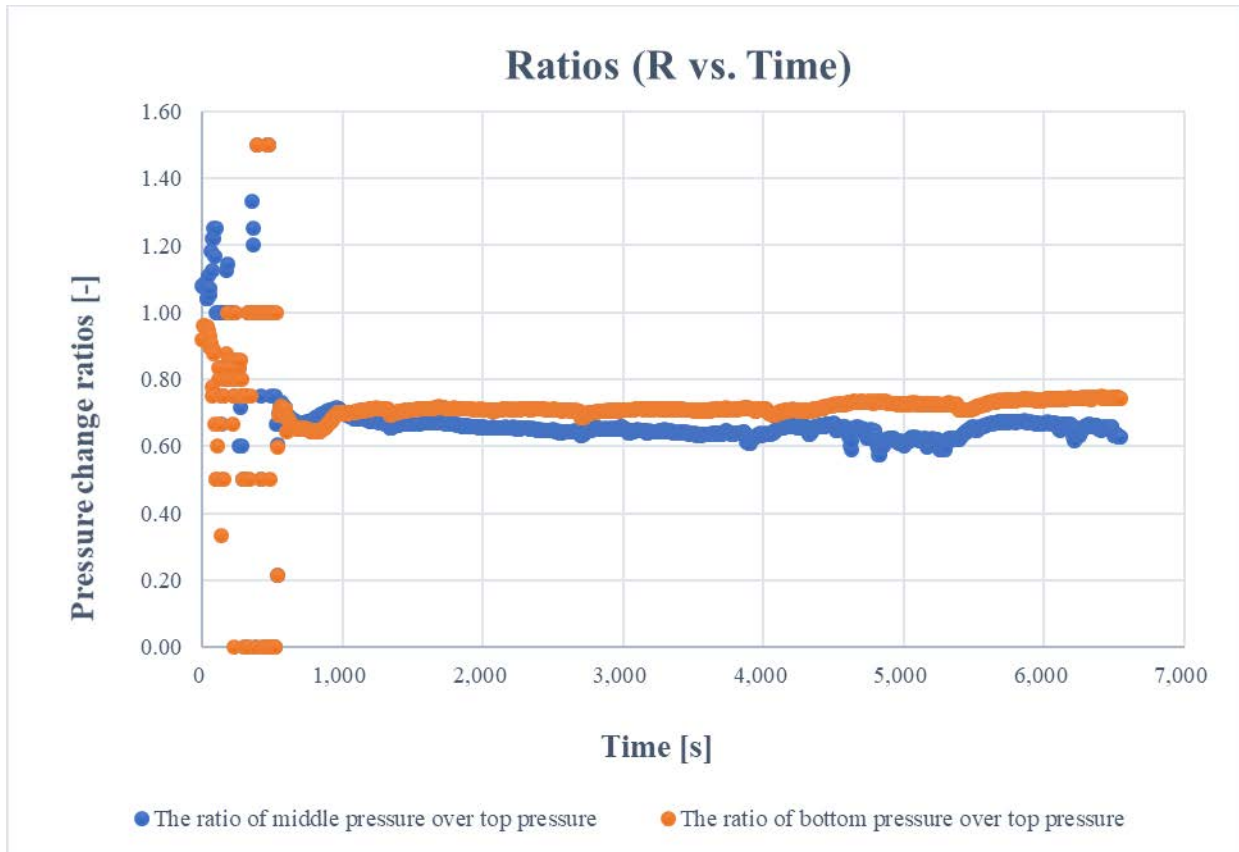
Figure 5.5 The ratio of middle pressure over top pressure and the ratio of bottom pressure over top pressure.

When the water flowed out from the injection screen, it was closest to the top transducer. These measurements or readings were expected to give the highest pressure values. With respect to the middle transducer readings, these measurements were further away from the injection screen. As a result, these readings were expected to be lower than those from the top transducer. Similarly, the pressure readings taken from the bottom transducer (furthest away from the injection screen) were expected to be lower than both the top and middle transducer pressure measurements.

Referring to Figure 5.4, the pressure differences were recorded in absolute pressure, taken in meters (of water column). As expected, the pressure differences from the top transducer were the highest, while the pressure differences recorded from the middle and bottom transducers were very close in value. Additionally, the measurements taken from the bottom transducer had slightly higher pressure differences than the pressure differences taken from the middle transducer. The pressure difference to the bottom traducer should be the lowest, but the test data proved contrary to this. This is attributed to the nonuniform compaction of the soil and/or piping present in the probe between the middle and bottom transducers.

In Figure 5.5, the ratios nicely stabilize after some minor initial turbulence, due to the filling of the water vessel and the changing of the water table. Ideally, the bottom ratio should be smaller than the middle ratio. The fact that they were about the same could be due to some piping along the

48

probe (high k connection between middle and bottom transducer locations). Therefore, the pressure data measured from the bottom was not used for any further calculations and analyses. A ratio of Mid/Top ≈ 0.6 was used to get the anisotropy ratio from Figure 5.6 below.
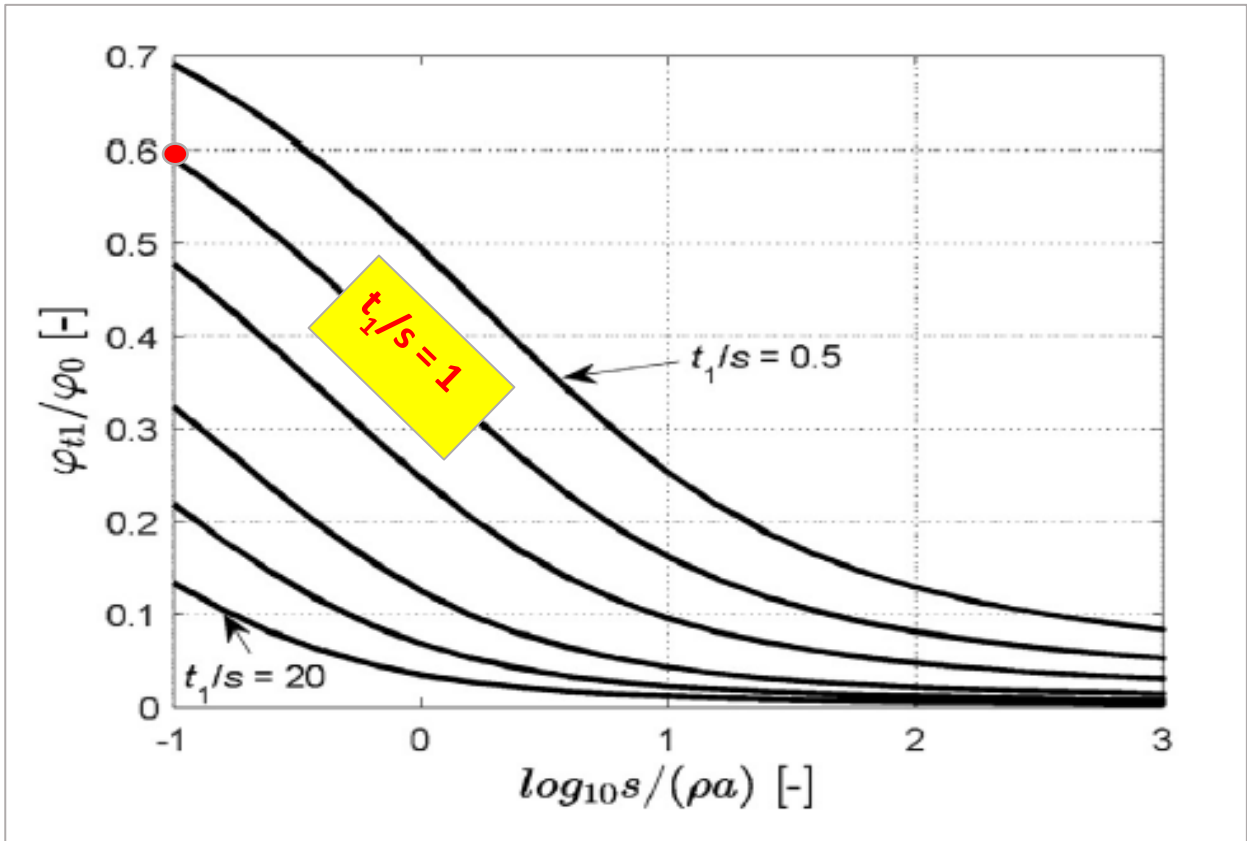
Figure 5.6   Normalized head $\varphi t1/\varphi 0$ (same as ΔPmiddle/ΔPtop) as a function of anisotropy ratio ρ for single injection from a lateral screen of length s with separate head monitoring at a distance t1 from the screen edge, is used to determine the ρ.

The probe geometry is listed in Chapter 2 and 3. The $s/a = 2$, $t_1/s = 1$ from probe geometry and $\varphi_{t1}/\varphi_{t2}$ (same as Rm) ≈ 0.6 from the ratio data for Mid/Top from Figure 5.6. Based upon Figure 5.6, the $\log_{10}[s/(\rho a)] = -1$ equation was used to find the red point, which gives $\rho = 20$. Based on the high ρ value, it also indicated some piping (high k connections) along the probe. By knowing $\rho = 20$, the relationship between k_v and k_h is determined by Equation 2-6, which results in $k_v = 400k_h$.
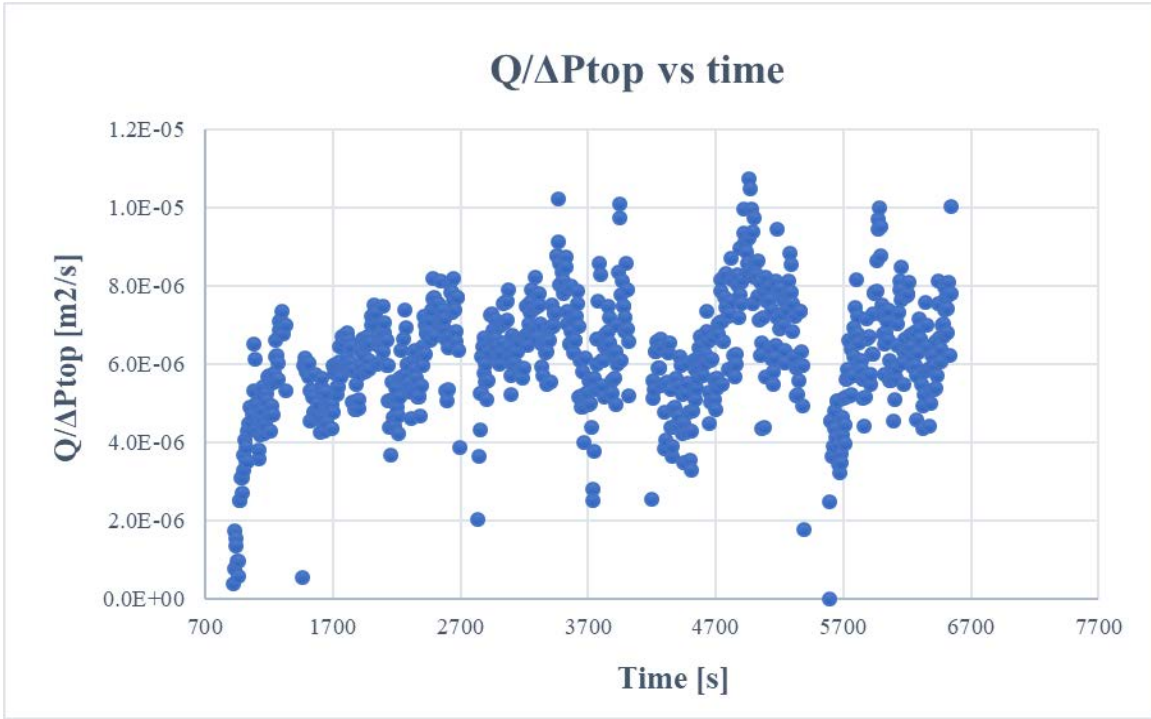
Figure 5.7 The flow rate of water vessel over the pressure difference, between top pressure and average background pressure, at 2-minutes intervals, Q/ΔPtop.
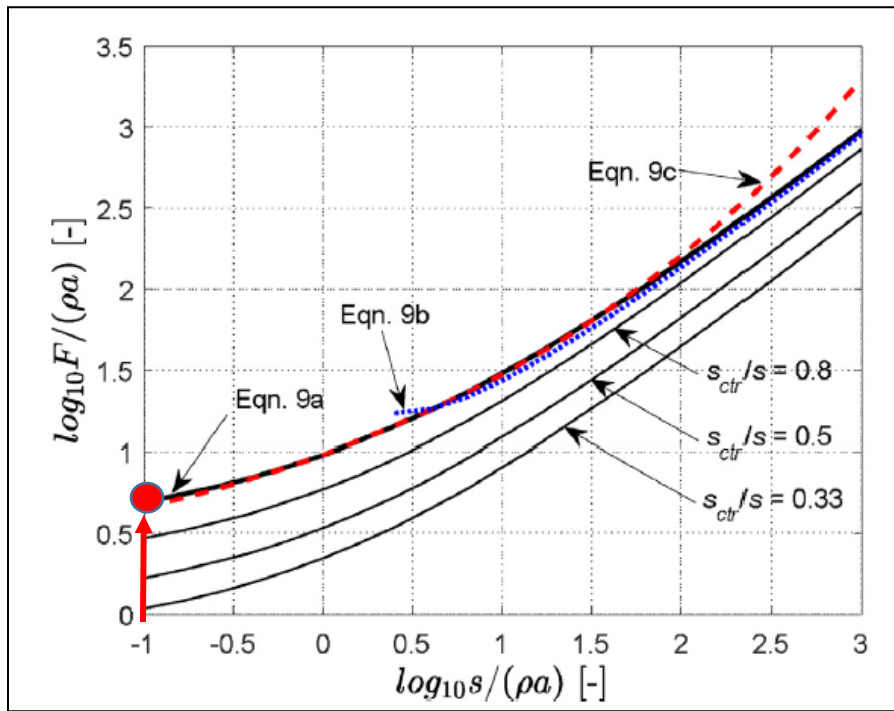
Figure 5.8 The shape factor, F, as a function of injection screen length s, probe radius a, and anisotropy ratio ρ.

There were two approaches to compute the shape factor, F. The first method was to use the shape factor chart to approximate F as shown in Figure 5.8. Using the $\log_{10}[s/(\rho a)] = -1$ from Figure 5-6 and applying it to $\log_{10}F/(\rho a)$ from Figure 5.8, it approximated 0.75 as the red dot. Therefore, F was equal to 2.3 m. The second method was to use equations to calculate the shape factor corresponding to the testing scenarios. Since $\log_{10}[s/(\rho a)] = -1$, it is in range of $-1 < \log_{10}s/\rho a < 2$ as indicated by the red dot/red arrow in the Figure 5.6. Equation 5-4b was then used to calculate F; F was equal to 2.69 m. The shape factors that were computed from the two methods were very close; however, the shape factor calculated from the equation was used for further analyses and calculations because it is considered more accurate.

Table 5.2.1 The Q/ΔPtop in two minutes interval for test 1, with calculated k_h and k_v.

| Test 1	Average Q/ΔP$_{top}$ (m^2/s)	k_h (m/s)	k_v (m/s)
1-5 mins	5.04E-06	1.87E-06	7.50E-04
5-10 mins	5.91E-06	2.20E-06	8.79E-04
10-15 mins	6.03E-06	2.24E-06	8.97E-04

Table 5.2.2 The Q/ΔPtop in two minutes interval for test 2, with calculated k_h and k_v.

Test 2	Average Q/ΔP$_{top}$ (m^2/s)	k_h (m/s)	k_v (m/s)
1-5 mins	6.19E-06	2.30E-06	9.20E-04
5-10 mins	6.70E-06	2.49E-06	9.97E-04
10-15 mins	7.23E-06	2.69E-06	1.08E-03

Table 5.2.3 The Q/ΔPtop in two minutes interval for test 3, with calculated k_h and k_v.

Test 3	Average Q/ΔP$_{top}$ (m^2/s)	k_h (m/s)	k_v (m/s)
1-5 mins	5.30E-06	1.97E-06	7.88E-04
5-10 mins	5.45E-06	2.03E-06	8.11E-04
10-15 mins	7.95E-06	2.96E-06	1.18E-03

Table 5.2.4 The Q/ΔPtop in two minutes interval for test 4, with calculated k_h and k_v.

Test 4	Average Q/ΔP$_{top}$ (m^2/s)	k_h (m/s)	k_v (m/s)
1-5 mins	5.10E-06	1.90E-06	7.58E-04
5-10 mins	6.83E-06	2.54E-06	1.02E-03
10-15 mins	6.34E-06	2.36E-06	9.43E-04

The $Q/\Delta P_{top}$ was calculated and shown in Figure 5.7 and Table 5.2; the F was 2.69 approximated from Equation 5-4b. Equation 5-5 was used to calculate horizontal conductivity, k_h, as shown in Table 5.2. The relationship equation between k_v and k_h is $k_v = 400k_h$. The large ratio (400) between k_v and k_h is the anisotropy ratio squared (ρ^2), which indicated some piping issues along the probe. This high ratio relationship equation causes the vertical permeability range to be two orders of magnitude higher than the vertical permeability range. Therefore, the vertical conductivity, k_v, was calculated based on k_h, shown in Table 5.2 as well. The range of horizontal conductivity was $1.90\times10^{-6} – 2.96\times10^{-6}$ m/s, and the range of vertical conductivity was $7.58\times10^{-4} – 1.18\times10^{-3}$ m/s.

5.4   CONCLUSIONS, POSSIBLE ERRORS, AND DISCUSSION

The FDOT test pit injection tests served to successfully validate the compatibility of the VAHIP PVC prototype probe with FDOT field equipment, such as injection vessel, hose and data acquisition, laptop connection and visualization. The adjustment of rising and lowering of the water table for the injection test was only for the FDOT test pit to compact the soil for the test. In future field tests, the water table will be the groundwater table in the field and need to be recorded. The test data used in the final analysis was from the fourth series of tests completed in the FDOT test pit. The first, second, and third series of tests failed due to water piping along the probe to the ground surface, which caused the PVC probe to record unreasonable data for determination of horizontal and vertical conductivity. There were several reasons that could have caused this problem and are identified below.

First, followed the FDOT test pit procedure (shown in Section 5.1), a hand auger was used to dig the hole for the PVC probe. The hole was slightly bigger than the probe. After inserting the probe, the soil had to be replaced in the annular space between the probe and the soil. A tamping rod and square hand tamper were used to compact the soil filling this annular space. Using this produce could have resulted in nonuniform compaction producing open spaces (large voids) between the probe and the soil, leading to piping issues along the PVC probe.

Second, due to the depth limitation of the FDOT test pit, the PVC probe had an embedment depth of 27 inches. The hydraulic gradients were directly proportional to the changing heads and it is inversely proportional to the water flowing path. The water flowing path in the test pit is from the injection screen to the embedment surface. For all the failed tests, the hydraulic gradients were too high at the surface due to the short water flowing path. This was the result of the FDOT test pit tests having a limited PVC probe depth, which caused high hydraulic gradients around the probe. This was observed as water suddenly broke the ground surface around the probe, causing a boiling condition. For the fourth series of tests, the water did not break the ground surface because the depth of the probe was inserted deeper and the head of the water vessel was lower. The high anisotropy ratio (ρ) calculated from the fourth test data indicated that there was still some piping (high k connections) along the probe, but it did not reach the surface of the soil. The unexpected issues with piping/upwelling would have occurred in the same way for any other probe type as well, thus, no further pit tests were needed.

Both issues will not occur in the future field test, where the steel probe is driven. The depth of driven probe will be deep enough (5 ft, 10 ft, etc. into the ground) to create low hydraulic gradients

to prevent any piping issues. In addition, the assumption is that the soil in the field test would be well compacted (native soil), and the probe will be driven or pushed into the ground. Therefore, there would be more intimate contact between the soil and probe which should limit piping issues.

CHAPTER 5

6. FABRICATION OF A STEEL PROBE

Several field injection tests were performed at the Florida Department of Transportation (FDOT) using the Vertical and Horizontal In situ Permeameter (VAHIP) steel probe. The specific location was in the backyard of the geotechnical test pit and next to the parking lots at FDOT in Gainesville, Florida. The field test location had a shallow groundwater table (around 5 to 8 feet below the ground surface), since there was a stormwater storage pond containing water right next to it. During testing periods, we often experienced thunderstorms, which helped keep the soil fully saturated at the testing location and a consistent shallow groundwater table during the testing period. The tests were performed in the saturated zone at the field test site. The compacted and saturated natural soil at the field site was used to test, analyze, and compute horizontal and vertical permeabilities.

6.1   THE OBJECTIVES OF VAHIP FIELD TEST

- Verify the proper performance of the steel probe;
- Modify the testing procedures based on issues encountered during lab and FDOT test pit experiments;
- Verify data transmission, real time visualization, and file storage from the steel probe readings;
- Analyze data, discuss test results, and compare test results from the lab test.

6.2   PROCEDURE

The procedure of field tests was similar to the tests in the FDOT test pit. The differences between tests at FDOT test pit and field test were: first, the proper compaction of the PVC prototype probe in the test pit was required, however, compaction was not needed for the field test because the steel probe was directly pushed into ground by the drill rig; second, the level of the water table at the test pit was adjustable for compaction and testing; third, field tests require a longer amount of time to calibrate and test because the soil is less permeable. The specific procedure of the tests at the test pit was listed in Task 5.d.

1. Follow instructions contained within the VAHIP Labview Program Manual (VAHIP Labview Program and power supply setup shown as in Figure 6.1)
   a) Confirm the computer, data acquisition module (DAQ), and sensors are functioning properly. A livestream should be visible on the computer.
   b) After confirmation, the test can be initiated.
2. Start test.
   a) Fill the falling head vessel with water to the 20-inch mark. Allow water to permeate into the soil.
   b) Remove all air voids within the probe and hose. This will require shaking the hose.
      i. Once you believe all of the air voids have been removed, the test can be started.

c) Fill the falling head vessel with water to the 21-inch mark and prepare to start recording when the water level approaches the 20-inch mark.
d) When ready, simultaneously start recording on the computer, start a stop watch, and mark the initial reading on the falling head vessel.
e) Mark a reading on the falling head vessel at every 5 minutes increment.
f) Conduct the test for 60 minutes.
g) At the conclusion of each test, record all data marked on the falling head vessel and erase the marks. Follow the Labview procedure to save all recorded data from the computer. This will conclude the test.
h) Repeat steps c through g three times. This will provide a saturation period of 60 minutes from the first test, and one or more individual, 60-minute tests can be used for analysis.

Figure 6.9 VAHIP Labview Program with power supply setup in field

Figure 6.10 The setup of field test in backyard of FDOT using the VAHIP steel probe.

6.3   DATA ANALYSIS

In order to assess vertical and horizontal permeability, the data recorded during the injection test was analyzed as follows. (The following analysis processes are analogous to the results from the test pit from Task 5.d).

1. The average background pressures (P_{top0}, $P_{middle,0}$, $P_{bottom,0}$) at a test location (depth) before starting injection were recorded at each transducer in units of meter of water column (Figure 6.3, green box).

2. The differences between average background pressures and measured pressures during injection from each transducer were found, shown in Figure 6.4:

$$\Delta P_{top} = P_{top} - P_{top,0} \tag{6-1a}$$

$$\Delta P_{middile} = P_{middle} - P_{middle,0} \tag{6-1b}$$

$$\Delta P_{bottom} = P_{bottom} - P_{bottom,0} \tag{6-1c}$$

3. The ratios of pressures at the middle transducer to the top transducer and the ratio of bottom transducer to the top transducer were calculated for later use, shown in Figure 6.5:

$$\text{Ratio middle, } R_m = \frac{\Delta P_{middle}}{\Delta P_{top}} \tag{6-2a}$$

$$\text{Ratio bottom, } R_b = \frac{\Delta P_{bottom}}{\Delta P_{top}} \tag{6-2b}$$

4. The flow rate of the water vessel in six-second intervals are shown in Figure 6.7. The dt was 6 seconds, which was the time interval for the VAHIP steel probe to take each reading/measurement:

$$Q = \frac{(\Delta P_{top,t=300s} - \Delta P_{top,t=0s}) \times A_{cross\ section}}{dt} \tag{6-3}$$

5. The anisotropy ratio ρ was found from Figure 6.6; s was the length of the lateral screen; and t_1 was the distance from the lateral screen to the nearest head monitoring location. φ_0 is the normalized head, it is equal to the difference of injection head and background head. Therefore, the φ_0 is same as the pressure difference (ΔP_{top}) on the top transducer. Once ρ is known, shape factor F and subsequently k_h and k_v are estimated from Equations 6-4 through 6-6.

For $\log_{10}(s/\rho a) > 0.5$:

$$\frac{F}{\rho a} \approx \frac{2\pi \frac{s}{\rho a}}{\ln \frac{s}{\rho a}} \tag{6-4a}$$

For $-1 < \log_{10}(s/\rho a) < 2$:

$$\frac{F}{\rho a} \approx 9.66\left[\left(\frac{s}{\rho a}\right)^{0.175}\right] \tag{6-4b}$$

6. Horizontal conductivity k_h, Q, ΔP_{top} in 5-minute intervals (300 seconds) are shown in Figure 1-6 and Table 1.2:

$$k_h = \frac{Q}{F\Delta P_{top}} \tag{6-5}$$

7. Vertical conductivity k_v:

$$\rho = \sqrt{\frac{K_v}{K_h}} \tag{6-6}$$

$$k_v = K_h \rho^2$$

6.4   ASSESSMENT OF HORIZONTAL AND VERTICAL CONDUCTIVITY
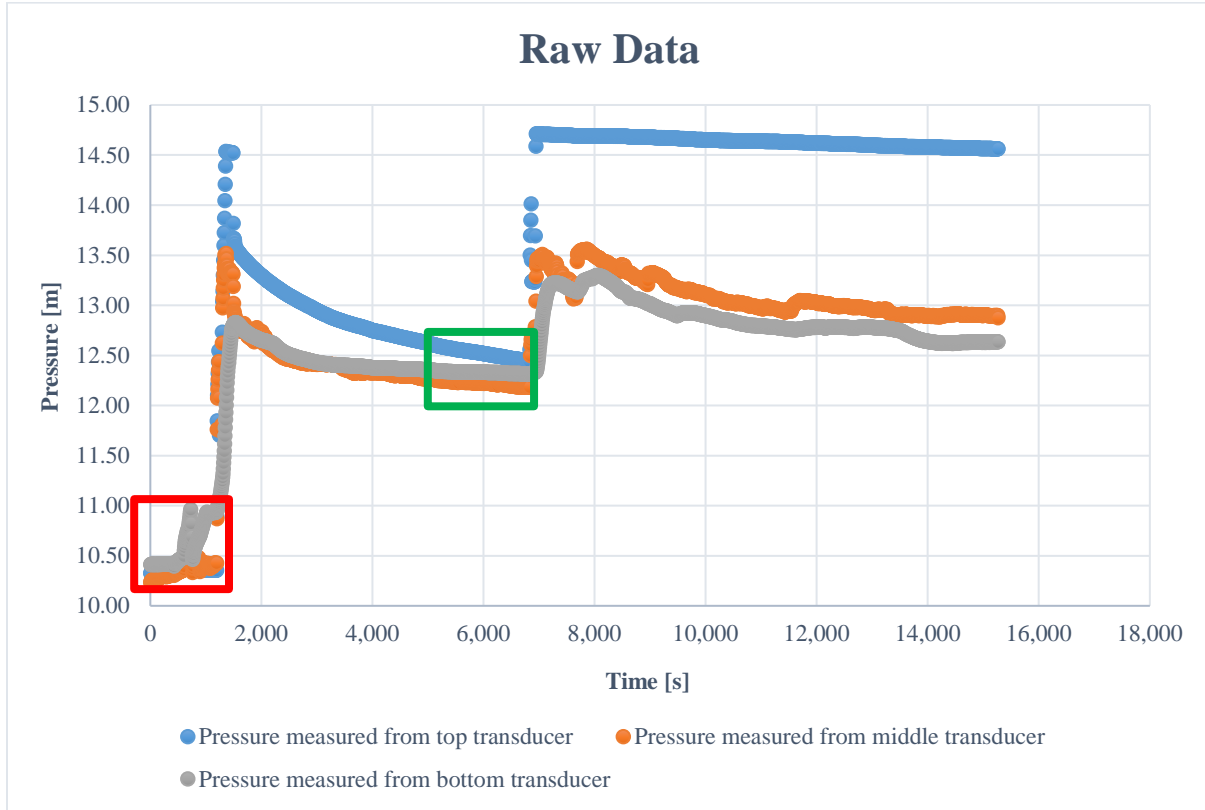
Figure 6.3 The raw data of the field test had two sets of data measured from the top, middle, and bottom transducers.

The measurements taken before the injection are shown in the red box, which measured atmosphere pressure. The average background pressures were taken after the calibration test are shown in the green box in Figure 6.3.

Table 6.1 The average background pressure of test pit measured from each transducer

$P_{top,0}$ (m)	$P_{middle,0}$ (m)	$P_{bottom,0}$ (m)
12.45	12.16	12.26

The pressures taken from each transducer include atmospheric pressure with measurement recorded in meters (of water column). Table 6.1 shows the average background pressure taken from each set of data. The average background pressure measured were 12.45 m, 12.16 m, and 12.26 m from the top, middle, and bottom transducers, respectively.
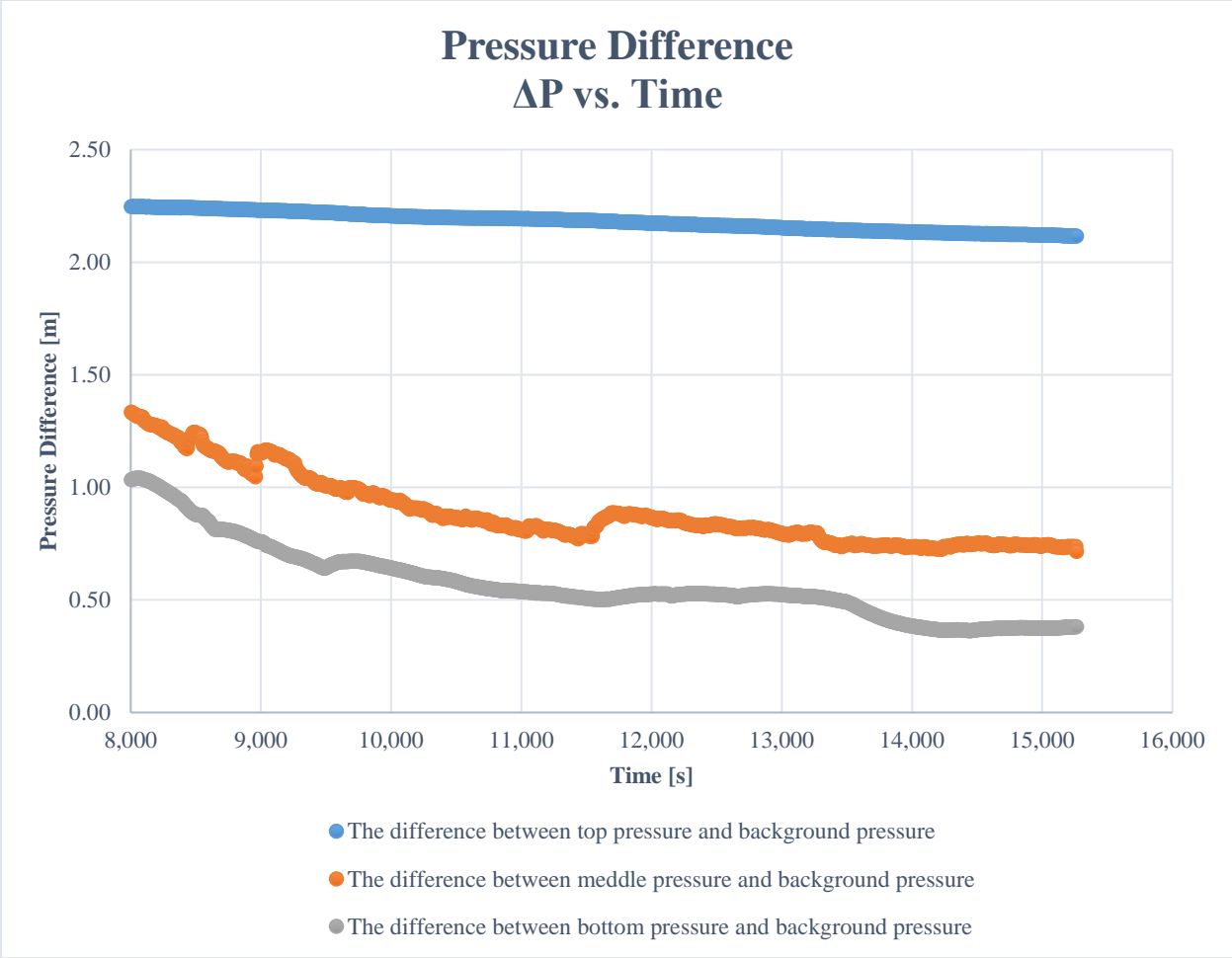
Figure 6.4 The difference between the average background pressure and the pressure measurements taken from all the transducers.

Head Ratios (R vs. Time)
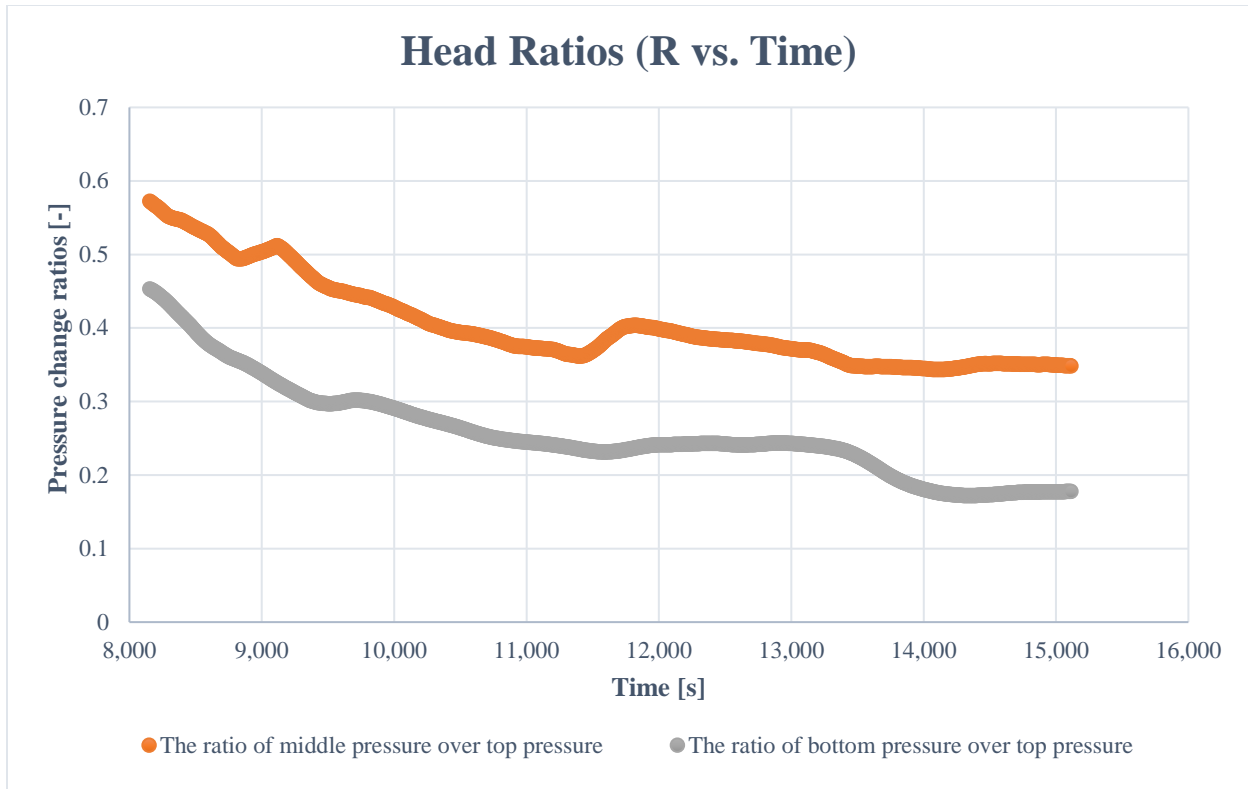
Figure 6.5 The ratio of middle pressure over top pressure shown in orange and the ratio of bottom pressure over top pressure shown in gray.

Referring to Figure 6.4, the pressure differences were recorded in absolute pressure, taken in meters (of water column). As expected, the pressure differences from the top transducer were the highest, while the pressure differences recorded from the middle and bottom transducers were remarkably close in value. Additionally, the measurements taken from the middle transducer had slightly higher pressure differences than the pressure differences taken from the bottom transducer. In theory, the pressure difference of the bottom traducer should be the lowest, the test data confirmed this.

In Figure 6.5, the ratios gradually decreased over time before the stabilizing. Ideally, both the middle and bottom ratios should remain relatively constant over time, and the bottom ratio should be smaller than the middle ratio. A ratio of Mid/Top ≈ 0.35 was used corresponding to the time period after approximately 13,500 seconds. The ratio of Mid/Top ≈ 0.35 was used to get the anisotropy ratio from Figure 6.6.

61
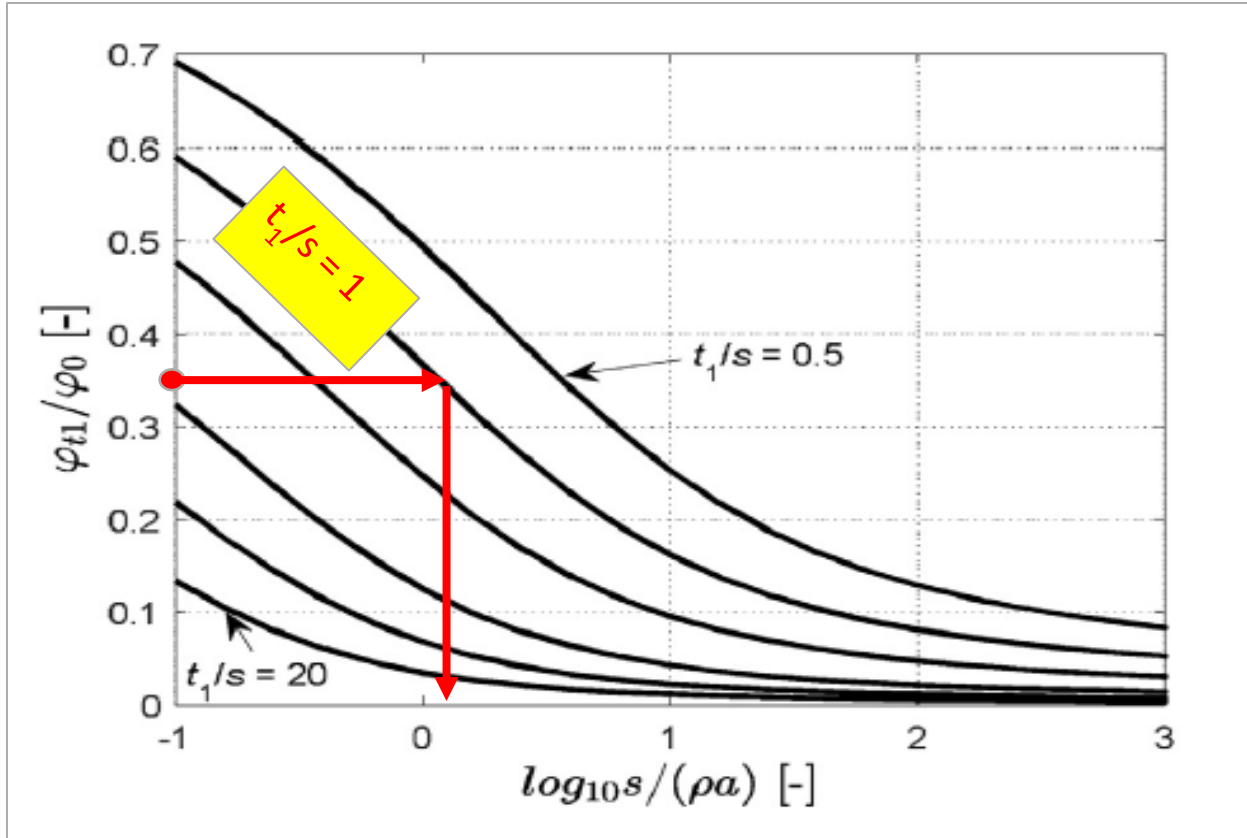
Figure 6.6 Normalized head $\varphi t1/\varphi 0$ (same as $\Delta P_{middle}/\Delta P_{top}$) as a function of anisotropy ratio ρ for single injection from a lateral screen of length s with separate head monitoring at a distance t_1 from the screen edge, is used to determine the ρ.

The probe geometry is listed in Chapter 2 and 3. The $s/a = 2$, $t_1/s = 1$ from probe geometry and $\varphi_{t1}/\varphi_{t2}$ (same as Rm) ≈ 0.35 from the ratio data for Mid/Top from the chart above. Based upon Figure 6.6, we find $\log_{10}[s/(\rho a)] = 0.2$ giving $\rho = 1.2$ and $k_v = 1.44 k_h$ from Equation 6-6.
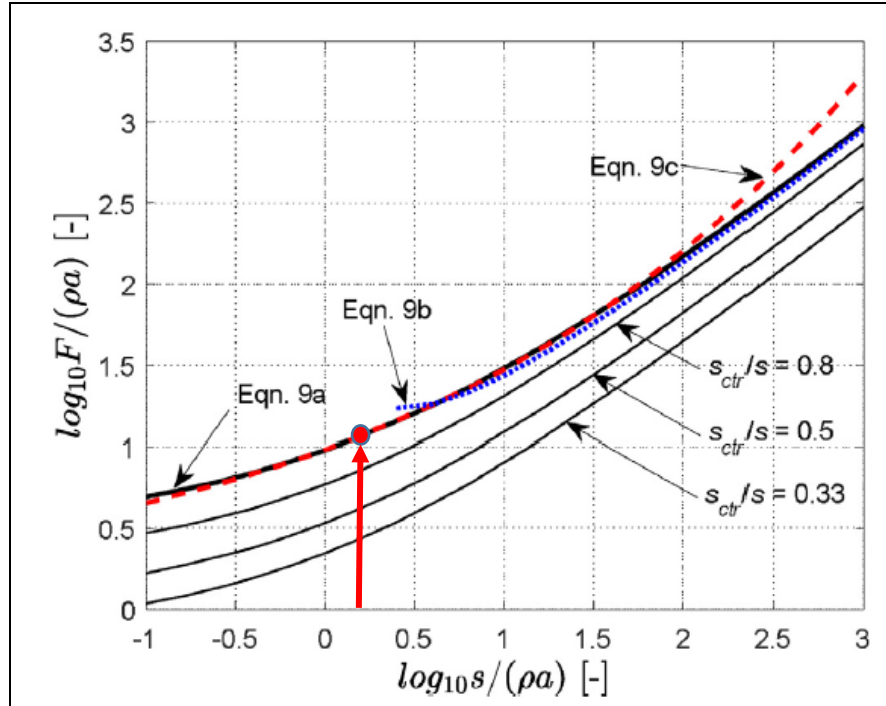
Figure 6.7   The shape factor, F, as a function of injection screen length s, probe radius a, and anisotropy ratio ρ.

There were two approaches to compute the shape factor, F. The first method was to use the shape factor chart to approximate F, as shown in Figure 6.8. Using the equation of $\log_{10}[s/(\rho a)] = 0.2$ from Figure 6.6 and applying it to $\log_{10}F/(\rho a)$ from the Figure 1-8, it approximated 1.1 as the red dot. Therefore, F was equal to 0.32 m. The second method was to use equations to calculate the shape factor corresponding to the scenarios. Since $\log_{10}[s/(\rho a)] = 0.2$, it is in range of $-1 < \log_{10}s/\rho a < 2$, as indicated by the red dot/red arrow in the Figure 6.7. Equation 6-4b was then used to calculate F=0.26 m. Even though the chart was developed from the same equations, the shape factor calculated from the equation is considered more accurate and was used for further analysis.

Table 6.2. The Q in six minutes interval for test, with calculated k_h and k_v.

Q (m³/s)	$\Delta P_{top, average}$ (m)	F (m)	ρ (-)	k_h (m/s)	k_v (m/s)
3.83E-07	2.18	0.26	1.2	6.65E-07	9.60E-07

The calculated flow rate of the test in six-minute intervals is 3.83E-07 m³/s, and the calculated shape factor is 0.26 m. The average of pressure difference between the top and background pressure in six-minute intervals was used to calculate the conductivity of 2.18 m. The anisotropy ratio is 1.2. In addition, with Equation 6-6, the relation between horizontal and vertical conductivity was determined as $k_v = 1.44k_h$. Using Equation 6-5, the horizontal conductivity (k_h) was calculated as 6.65E-07 m/s, and the calculated vertical conductivity (k_v) was 9.60E-07 m/s.

6.5   CONCLUSIONS AND POSSIBLE LIMITATIONS

The VAHIP steel probe injection field tests in the backyard of FDOT test pit took longer than the test pit tests. The field tests operated during a thunderstorm period, therefore, only one successful field test was obtained. The ground water table at the field test location was shallow, with a depth of 7 ft. The VIHIP steel probe was directly pushed into the ground by a drill rig. The steel probe was tested under the ground water table, which assumes that the soil was fully saturated. The data of the field test was successful recorded and saved for calculation and analysis. As there was only one successful field test data collected, the conclusion and discussion of the field test was based on that, along with the possible limitations.

From the field test data, the calculated horizontal conductivity (k_h) is 6.65E-07 m/s, and the calculated vertical conductivity (k_v) is 9.60E-07 m/s. The soil layer tested at the field test location had a low permeability, from which the soil was classified as a silty or clayey material, which would explain why the field tests took a longer time to complete. The values of horizontal conductivity and vertical conductivity are very close, indicating that the test soil may be relatively isotropic.

Possible limitations that may require further attention include effects of soil clogging and the loosening of the rubber stoppers holding the pressure transducers.

Soil clogging: The soil clogging of the injection points/areas of the VAHIP steel probe has been a constant problem since the first generation of the probe design. Every design of the probe has tried to solve this clogging issue, but none has been effective. The geometry of the injection points/areas, their location on the probe, the quantity of these points/areas were all taken into consideration. The probe used in this test has injection screens. The details of this screen were reported in Task 5.b, with thorough drawings and explanations. This attempt at solving the soil clogging problem, however, was still ineffective. After each test, when the probe was taken out of the ground, there would be soil clogged in the injection screens. A grill brush was used to clean the injection screens and water was poured into the probe to clean out the inside. Whenever this task was performed, there would always be soil in the water that flushed out, and any soil infiltrating the probe would restrict water flow. It is noted that the porous rings around the inlets of the middle and bottom pressure chambers did not suffer from significant smearing problems. This indicates that the deployment of a longer porous filter ring around the injection screen may be a possible solution to this limitation, which is beyond the scope of the present project.

Loosening of the rubber stopper: Three transducers were each placed with a cable inside the VAHIP steel probe at the top, middle, and bottom chambers, which are held in place by three rubber stoppers. The stoppers have holes where the transducer cables passed through. The purpose of using rubber stoppers was to hold the transducers and cables in place while preventing water from flowing between different chambers of the probe. Detailed drawings and explanations are shown in Chapter 5. During the field tests, the top transducer would often come out of the probe and it was difficult to readjust the transducer into the correct orientation. As a result of this, the rubber stopper's hole may have loosened. This means that during testing, the transducers could potentially move from their original locations. The loosening of the stoppers could also cause water leakage between different pressure chambers, thus partially distorting measurements. It is

suggested to switch to a new stopper with a smaller hole, which would hold the cable tighter and improve accuracy.

DATA RECORDED DURING INJECTION TESTS

Table A.1 Data recorded during injection tests for the scenario 1 (the rest of the data is presented in Table 1.7)

n	Top transducer		Middle transducer		Bottom transducer		Weight				
	Voltage (V)	Height of water (cm)	Voltage (V)	Height of water (cm)	Voltage (V)	Height of water (cm)	of water (g)	t (s)	Q (cm³/s)	H (cm)	Δ (cm)
1	5.061	41.13	5.120	55.68	5.220	68.75				88.44	
2	5.107	50.83	5.140	59.90	5.224	69.60	529.72	60	8.83	88.44	0.00
3											
	5.061	41.13	5.120	55.68	5.220	68.75				88.44	
4	5.114	52.30	5.140	59.90	5.223	69.39	549.92	60	9.17	88.44	0.00
5											
	5.070	43.02	5.120	55.68	5.218	68.33				88.44	
6	5.127	55.04	5.150	62.00	5.228	70.44	662.88	60	11.05	88.44	0.00
7	5.075	44.08	5.130	57.79	5.225	69.81				88.44	
8	5.141	58.00	5.160	64.11	5.233	71.50	778.29	60	12.97	88.44	0.00
9	5.078	44.71	5.130	57.79	5.231	71.07				88.44	
10	5.156	61.16	5.160	64.11	5.241	73.18	772.98	50	15.46	89.04	0.60
11	5.080	45.13	5.130	57.79	5.240	72.97				89.04	
12	5.161	62.22	5.165	65.17	5.245	74.03	726.95	45	16.15	89.04	0.00
13	5.075	44.08	5.130	57.79	5.242	73.39				88.44	
14	5.124	54.41	5.150	62.00	5.247	74.45	589.73	60	9.83	88.74	0.30
15	5.075	44.08	5.130	57.79	5.247	74.45				88.44	
16	5.110	51.46	5.140	59.90	5.250	75.08	504.40	60	8.41	88.44	0.00

Note: n= odd number, represent readings before injection. n= even number are readings during injection.
H is the level of water inside the barrel and Δ is difference between H before and during injection

Table A.2 Data recorded during injection tests for the scenario 2 (the rest of the data is presented in Table 1.9)

n	Top transducer Voltage (V)	Height of water (cm)	Middle transducer Voltage (V)	Height of water (cm)	Bottom transducer Voltage (V)	Height of water (cm)	Weight of water (g)	t (s)	Q (cm³/s)	H (cm)	Δ (cm)
1	5.103	35.64	5.143	48.30	5.253	67.91				85.54	
2	5.159	47.45	5.223	65.17	5.272	71.92	719.61	40	17.99	86.94	1.40
7	5.142	43.87	5.140	47.66	5.251	67.49				86.04	
8	5.258	68.33	5.160	51.88	5.265	70.44	653.25	45	14.52	86.84	0.80
9	5.166	48.93	5.140	47.66	5.251	67.49				86.04	
10	5.323	82.04	5.158	51.46	5.263	70.02	665.29	50	13.31	86.59	0.55
11	5.172	50.19	5.140	47.66	5.250	67.28				86.14	
12	5.204	56.94	5.150	49.77	5.258	68.96	516.89	55	9.40	86.54	0.40
13	5.125	40.28	5.140	47.66	5.251	67.49				85.94	
14	5.184	52.73	5.170	53.99	5.268	71.07	769.45	45	17.10	86.84	0.90
15	5.125	40.28	5.140	47.66	5.251	67.49				85.94	
16	5.178	51.46	5.160	51.88	5.265	70.44	607.51	45	13.50	86.64	0.70
17	5.169	49.56	5.140	47.66	5.252	67.70				85.94	
18	5.212	58.63	5.160	51.88	5.265	70.44	630.82	50	12.62	86.54	0.60

Note: n= odd number, represent readings before injection. n= even number are readings during injection.
H is the level of water inside the barrel and Δ is difference between H before and during injection

Table A.3 Data recorded during injection tests for scenario 3 (the rest of the data is presented in Table 1.11)

n	Top transducer Voltage (V)	Height of water (cm)	Middle transducer Voltage (V)	Height of water (cm)	Bottom transducer Voltage (V)	Height of water (cm)	Weight of water (g)	t (s)	Q (cm³/s)	H (cm)	Δ (cm)
1	5.047	26.36	5.105	43.66	5.192	56.31				88.44	
2	5.117	41.13	5.150	53.15	5.208	59.68	754.64	50	15.09	88.94	0.50
7	5.055	28.05	5.105	43.66	5.195	56.94				88.94	
8	5.110	39.65	5.140	51.04	5.205	59.05	757.16	55	13.77	89.04	0.10
9	5.056	28.26	5.110	44.71	5.194	56.73				89.04	
10	5.096	36.70	5.140	51.04	5.202	58.42	679.32	60	11.32	88.94	-0.10
11	5.053	27.63	5.110	44.71	5.216	61.37				88.84	
12	5.076	32.48	5.120	46.82	5.215	61.16	386.61	60	6.44	88.64	-0.20
13	5.051	27.21	5.110	44.71	5.213	60.74				88.64	
14	5.069	31.00	5.120	46.82	5.213	60.74	284.36	60	4.74	88.44	-0.20
15	5.051	27.21	5.110	44.71	5.211	60.32				88.89	
16	5.091	35.64	5.130	48.93	5.212	60.53	607.58	60	10.13	88.84	-0.05

Note: n= odd number, represent readings before injection. n= even number are readings during injection.
H is the level of water inside the barrel and Δ is difference between H before and during injection

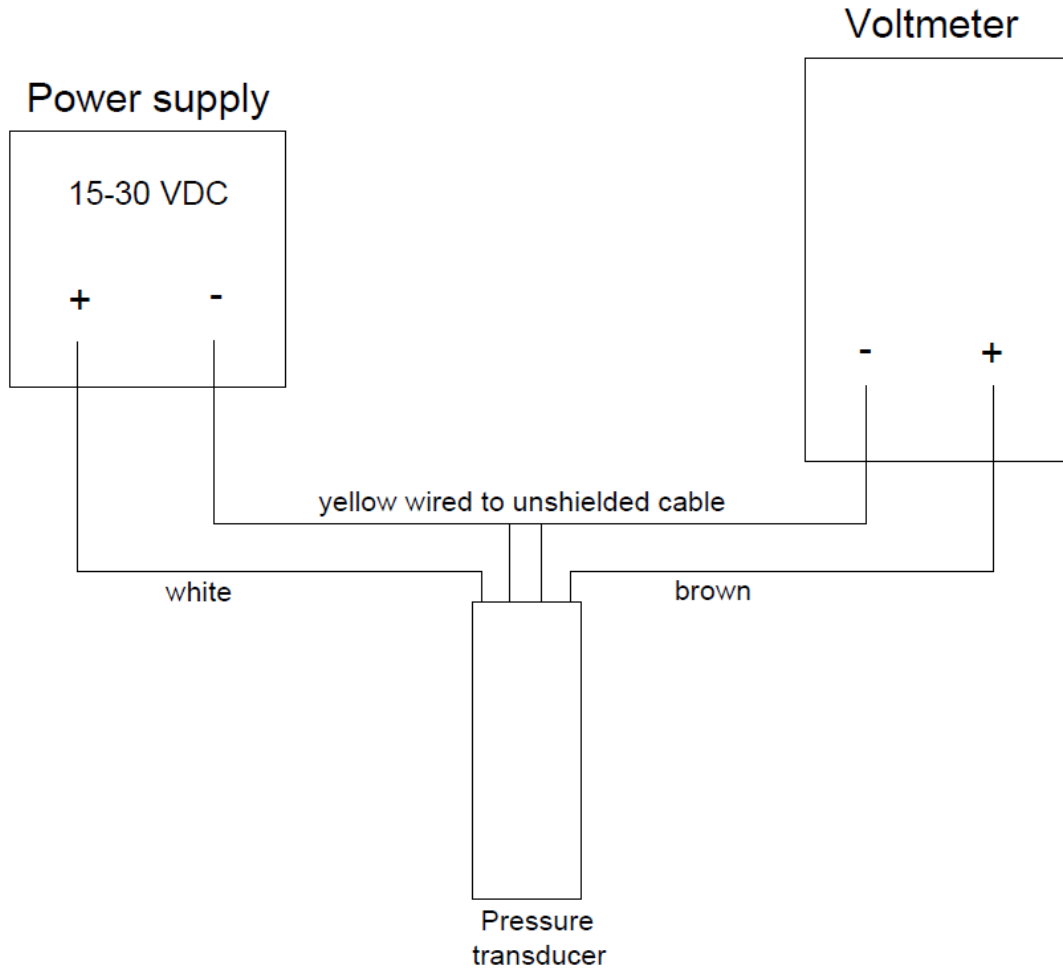# PRESSURE TRANSDUCERS WIRE DIAGRAM

Figure B.1 Pressure transducers wire diagram (Figure courtesy of author)

REFERENCES

Klammler, H., L. Layton, B. Nemer, K. Hatfield, A. Mohseni. 2017. *Theoretical aspects for estimating anisotropic saturated hydraulic conductivity from in-well or direct-push probe injection tests in uniform media.* Advances in Water Resources, 104, 242-254.

Klammler, H., K. Hatfield, B. Nemer, S. Mathias. 2011. *A trigonometric interpolation approach to mixed type boundary problems associated with permeameter shape factors*. Water Resources Research, 47, W03510.